

Ludmil Drenchev

Jerzy J. Sobczak

Formation of Graded Structures and Properties in Metal Matrix Composites by use of Electromagnetic Field



Instytut Odlewnictwa
Foundry Research Institute

Ludmil Drenchev

Jerzy J. Sobczak

Formation of Graded Structures and Properties in Metal Matrix Composites by use of Electromagnetic Field

This project is funded by the Ministry of Education, Youth and Science of Bulgaria within the frame of a Sabbatical Program of the National Scientific Fund at the Ministry and was executed in the Foundry Research Institute, Krakow, Poland (03 May 2010–02 January 2011)

Computer typesetting: Agnieszka Fiutowska
Cover page design: Jan Witkowski, janwi.com

© Copyright by Instytut Odlewnictwa, Kraków 2010

ISBN 978-83-88770-55-5

Edited by:
Foundry Research Institute
Zakopianska 73
30-418 Krakow, Poland
www.iod.krakow.pl

Printing and binding:
Foundry Research Institute

Contents

Foreword.....	7
I. Introduction	9
II. Lorentz force in action	14
III. Project aim, objectives and activities.....	29
IV Methodology, equipment and experiments	32
V. Expected results and their practical applications	58
Symbols	60
References	61

Abstract

The aim of this publication is to outline briefly the idea for manipulation of gravity effects in electroconductive liquids by means of Lorentz force. Some initial results obtained in the Foundry Research Institute (FRI) in Cracow, related with practical utilization of this idea, are presented. Attention has been focused only on the force generated by simultaneous action of external constant electric and magnetic fields. Applied aspects of this idea are discussed, basing on the production of inhomogenous metal matrix composites.

At the beginning, the physical nature of Lorentz force is analyzed. The main algebraic and differential equations, which describe the basic physical phenomena taking place in metallic melt during solidification in the field of Lorentz force are also given. The experimental equipment designed and produced in FRI and its technical parameters are described. Numerous experiments with model suspensions have been carried out to demonstrate the potential of the approach considered. Some important experiments with trade metal matrix composite F3S.108 (DURALCAN) have been conducted to demonstrate the possibilities for control of sedimentation processes during solidification and production of functionally graded metal matrix composites. The plan of the experimental work and its aims are discussed in detail. At the end, the expected results and their possible applications in near future are argued.

Streszczenie

Celem niniejszej publikacji było przedstawienie koncepcji sterowania efektem grawitacji w cieczach elektroprowadzących dzięki zastosowaniu siły Lorentza. Przedyskutowano wyniki uzyskane wstępnie w Instytucie Odlewnictwa w Krakowie, dotyczące praktycznego wykorzystania tej koncepcji. Główny nacisk położono na zastosowanie siły generowanej przez jednoczesne oddziaływanie zewnętrznego stałego pola elektrycznego i magnetycznego. Aplikacyjny aspekt tej koncepcji omówiono w oparciu o proces wytwarzania gradientowych (w tym niejednorodnych) kompozytów o osnowie metalowej.

Na wstępie przeanalizowano fizyczne aspekty oddziaływania siły Lorentza. Podano również główne równania algebraiczne i różniczkowe, opisujące podstawowe zjawiska fizyczne zachodzące podczas krzepnięcia ciekłego metalu w polu działania siły Lorentza. Opisano aparaturę doświadczalną zaprojektowaną i wykonaną w Instytucie Odlewnictwa wraz z podaniem jej głównych parametrów technicznych. Opisano liczne eksperymenty własne z zastosowaniem modelowych zawieszin dla wykazania potencjalnych możliwości zaprezentowanej metody. W kilku istotnych doświadczeniach wykorzystano przemysłowe kompozyty o osnowie metalowej takie, jak F3S.10S (DURALCAN). Głównym celem tych doświadczeń było wykazanie możliwości kontrolowania procesu sedymentacji cząsteczek podczas krzepnięcia i wytwarzania funkcjonalnie gradientowych kompozytów o osnowie metalowej. Omówiono szczegółowo plan prac doświadczalnych i cel ich prowadzenia. W części końcowej przeanalizowano znaczenie oczekiwanych wyników oraz możliwości ich praktycznego wykorzystania w kolejnych etapach badań.

Foreword

During the last three years, in the Foundry Research Institute (FRI), many experiments related to manipulation of gravity effects by application of Lorentz force were carried out. Objects of interest were electroconductive liquids such as particle reinforced cast metal matrix composites and some salt-water solutions. The main aim of these experiments was establishment of basic quantitative relations between the processing parameters and various effects arising in electroconductive liquids in the field of Lorentz force. These experiments were also very useful for the design of experimental equipment and development of technology for the ceramic mould preparation. The preliminary work outlines the areas of future research and possible application of the results obtained. The design and assembly of the experimental equipment as well as all the experiments have been fully performed by Wojciech Leśniewski, M.Sc., from FRI. Special merit for a valuable contribution to the experimental work goes to Piotr Wieliczko, M.Sc., also from FRI. The project titled "Formation of Graded Structures and Properties in Metal Matrix Composites by Use of Electromagnetic Fields" appears as a logical continuation of the work which has been done in FRI till now. This project forms part of a Sabbatical Program of Prof. Ludmil Drenchev from the Institute of Metal Science at Bulgarian Academy of Sciences. It is funded by the Bulgarian Ministry of Education, Youth and Science and will be entirely executed in the Foundry Research Institute, Krakow, Poland.

Słowo wstępne

W ciągu ostatnich trzech lat w Instytucie Odlewnictwa przeprowadzono szereg eksperymentów związanych ze sterowaniem efektem grawitacji dzięki zastosowaniu siły Lorentza. Celem badań były ciecze elektroprowadzące, takie jak umacniane cząsteczkami ciekłe kompozyty o osnowie metalowej i niektóre wodne roztwory soli. Celem głównym eksperymentów było ustalenie podstawowych ilościowych współzależności pomiędzy parametrami procesu obróbki kompozytów i różnymi zjawiskami, które zachodzą w cieczech elektroprowadzących w polu działania siły Lorentza. Przeprowadzone eksperymenty były bardzo przydatne również podczas projektowania aparatury doświadczalnej i opracowania technologii przygotowania form ceramicznych. Badania wstępne wyznaczają zakres przyszłych prac i ewentualnego praktycznego wykorzystania wyników. Projektowanie i montaż aparatury doświadczalnej, jak również wszystkie eksperymenty zostały wykonane przez Wojciecha Leśniewskiego z Instytutu Odlewnictwa. Szczególne wyrazy uznania za cenny wkład w prace doświadczalne należą się Piotrowi Wieliczko, zatrudnionemu również w Instytucie Odlewnictwa. Projekt zatytułowany „Powstawanie struktur gradientowych i właściwości w kompozytach o osnowie metalowej dzięki zastosowaniu pola elektromagnetycznego” stanowi logiczną kontynuację prac, które zostały zrealizowane do chwili obecnej w Instytucie Odlewnictwa. Omawiany tu projekt stanowi część programu badań prowadzonych przez Prof. Ludmila Drencheva z Instytutu Metaloznawstwa Bułgarskiej Akademii Nauk. Program ten finansowany przez Ministerstwo Edukacji, Młodzieży i Nauki Bułgarii został przewidziany do pełnej realizacji w Instytucie Odlewnictwa w Krakowie.

I. Introduction

Originally, Lorentz Force (LF) is determined as the force which acts on a moving point electrical charge in crossed electric and magnetic fields and is defined by the following relation:

$$\mathbf{F}^L = q(\mathbf{E} + \mathbf{v} \times \mathbf{B}) \quad (1)$$

Hendrik Lorentz defined this force in 1892 [1], but in fact it was introduced in another form by James Clerk Maxwell (when Lorentz was still a young boy) in 1861 in a paper entitled: *On Physical Lines of Force*, equation (77), and in 1864 in a paper entitled: *A Dynamical Theory of the Electromagnetic Field*, equation (D), as one of the original eight Maxwell's equations. The equation (77) can be considered a predecessor of the modern Lorentz force equation (1). The currently used term "Maxwell's equations" comprises Maxwell's theory reformulated by Oliver Heaviside, and does not include the Lorentz force. Now it is associated with Maxwell's equations as a separate and essential law which expresses the effect of electric and magnetic fields on a charged point particle.

Let us consider a region in the space with moving electrical charges. All electroconductive mediums such as metals and alloys (solid or liquid), plasma, electrolytes and others possess electrically charged particles concentrated in certain space volume. If this volume is immersed in magnetic field, all the moving charged particles will be exerted of a force according to (1). The concentration of electrical free charges in mediums of practical interest is relatively high (in case of metals and alloys the electron density is about $10^{28}/\text{m}^3$) and they can be considered a "sea" of free electrical charges (electrons/ions).

The equation (1) consists of two components: electric, $q\mathbf{E}$, and magnetic, $q\mathbf{v} \times \mathbf{B}$. For a continuous medium with free electrical charges of the density n equation (1) can be modified as follows:

$$\mathbf{f}^L = nq\mathbf{E} + nq\mathbf{v} \times \mathbf{B} \quad (2)$$

where $\mathbf{f}^L = n\mathbf{F}^L$ is the volume density of LF. In the case of metallic medium $|\mathbf{E}| \ll |\mathbf{v} \times \mathbf{B}|$ and the first term in (2) can be neglected which leads to

$$\mathbf{f}^L = \mathbf{j} \times \mathbf{B} \quad (3)$$

where $\mathbf{j} = nq\mathbf{v}$ is the current density. Usually, in the case of metals, metallic materials and electroconductive liquids (which are of practical interest in this project), the term “Lorentz force” is referred to the magnetic component. Sometimes this is more convenient just because this component is responsible for the phenomena considered, for example, the force that acts on a current-carrying wire in a magnetic field. In what follows, the term “Lorentz force” will refer only to the expression of its magnetic component according to (3).

According to the differential form of Ohm’s law

$$\mathbf{j} = \sigma \mathbf{E} \quad (4)$$

Combining (3) and (4) we obtain

$$\mathbf{f}^L = \sigma \mathbf{E} \times \mathbf{B} = \sigma \mathbf{L} \quad (5)$$

The last formula defines a field (Lorentz field) with strength $\mathbf{L} = \mathbf{E} \times \mathbf{B}$ at each point of the area considered. The LF density is proportional to the specific electrical conductivity at this point and the field strength \mathbf{L} , as given by (5). It should be mentioned that the field defined is not related explicitly with electrical charges but with the electrical conductivity of an object “embedded” in this field. In all cases of practical interest, Lorentz field exists together with the gravity field. These two fields have different sources but they are very similar.

Let us consider a spherical solid particle of radius r_0 in electroconductive liquid, and let us assume the liquid is subjected to simultaneous action of gravity and Lorentz field. The forces that are applied on the particle can be listed as shown in Table 1.

Table 1. Forces generated in gravity and Lorentz fields acting on liquid and moving solid particle

Forces	In gravity field	In Lorentz field
Due to "charges" of particle	$\mathbf{F}_P^G = -\rho_P V_P \mathbf{g}$	$\mathbf{F}_P^L = -\sigma_P V_P \mathbf{L}$
buoyant	$\mathbf{F}_B^G = \rho V_P \mathbf{g}$	$\mathbf{F}_B^L = \sigma V_P \mathbf{L}$
Stokes'	$\mathbf{F}_S = -6\pi\eta_0 r_0 \mathbf{v}$	

Here V_p is the volume of the particle, ρ is the density of the liquid, ρ_P is the particle density, σ is the electrical conductivity of the liquid, σ_P is the electrical conductivity of the particle, η_0 is the dynamic viscosity of the liquid, and $\mathbf{v} = \mathbf{v}(t)$ is the velocity of the particle. A similarity between the gravity field and Lorentz field can be easily seen in Table 1. The gravity force is proportional to the gravity "charge" called mass, $\rho_P V_P$, but LF is proportional to the specific "charge", $\sigma_P V_P$.

Using the above expressions, Newton's law related to the particle considered can be written in the following form:

$$m_P \frac{d\mathbf{v}}{dt} = \mathbf{F}_B^G + \mathbf{F}_P^G + \mathbf{F}_B^L + \mathbf{F}_P^L + \mathbf{F}_S = (\rho - \rho_P)V_P \mathbf{g} + (\sigma - \sigma_P)V_P \mathbf{L} - 6\pi\eta_0 r_0 \mathbf{v}, \quad (6)$$

$\mathbf{v} = \mathbf{v}(t)$

The first term in the right side of the last equation is the gravitational Archimedes force applied to the particle (inclusion), the second term is Archimedes force arising in Lorentz field, and the last one is the drag force.

This vector equation can be written also as a system of three scalar ordinary differential equations for the three components of velocity, $\mathbf{v} = (v_x, v_y, v_z)$. In the case considered here, see Fig. 1, $v_x=0$ and $v_y=0$. Equation (6) is transformed into

$$m_P \frac{dv_z}{dt} = (\rho - \rho_P)V_P g + (\sigma - \sigma_P)V_P L - 6\pi \eta_0 r_0 v_z \quad (7)$$

This equation can be written in the form

$$\frac{dv_z}{dt} + Av_z = C \quad (8)$$

where the coefficients assume the following form

$$A = 6 \pi \eta_0 r_0 \quad (9)$$

$$C = (\rho - \rho_P)V_P g + (\sigma - \sigma_P)V_P L \quad (10)$$

Equation (8) has an analytical solution, which in the case of an initial condition $v_z(0) = 0$ assumes the following form:

$$v_z = v_{z,0} [1 - \exp(-6\pi \eta_0 r_0 t)] \quad (11)$$

where the terminal velocity, $v_{z,0}$, of the particle is

$$v_{z,0} = \frac{2r_0^2}{9\eta_0} [(\rho - \rho_P)g + (\sigma - \sigma_P)L] \quad (12)$$

On the basis of this analytical solution one can determine the position of a particle in melt as a function of time.

There are some essential differences between the gravity field and Lorentz field. First of all, the intensity of the gravity field is almost constant over

Earth's surface and cannot be controlled. *Vice versa*, the intensity of Lorentz field can be simply varied by changing the values of the magnetic and/or electric fields. Additionally, its direction can be also varied, since the directions of the applied electric and magnetic fields can be handled easily. The LF can be directed in parallel or opposite to the gravity force, thus amplifying, reducing or even inverting the gravity effect, as is shown in Fig. 1. Let it be mentioned that the Lorentz field does not affect gravity and does not change in

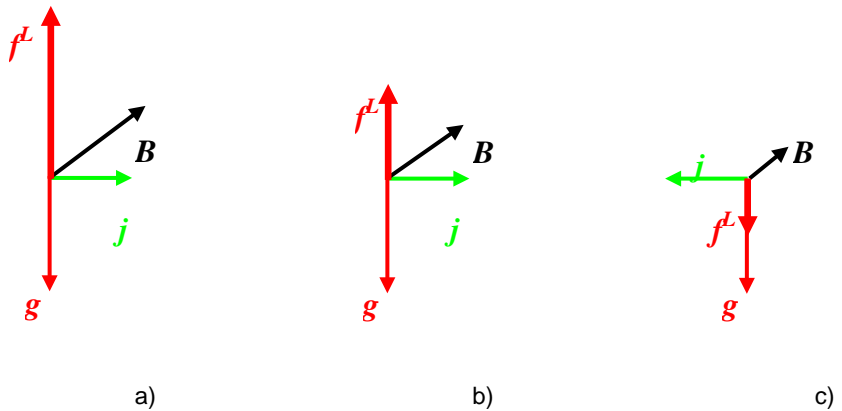


Figure 1. Possible configuration of magnetic and electric fields providing: a) apparent antigravity; b) apparent microgravity or zero gravity; and c) apparent supergravity

any degree the gravity acceleration. The Lorentz field is an additional field acting together with the gravity. The results of this joint action can be described as apparent supergravity, apparent microgravity and apparent antigravity, Fig. 1.

Manipulation and control of gravity effects is very important for various technologies which use liquid phase processing. One typical example is production of particle reinforced cast Metal Matrix Composites (MMCs) and especially Functionally Graded Materials (FGMs). Scientists and engineers are only at the beginning of large theoretical and experimental investigations in this area and good results, especially for graded cast materials, are not so close to practical implementations. Efficient application of Lorentz force in the process of structure formation of MMCs seems to be the most promising approach for production of cast FGMs. This is the main reason which provokes activities in the project here discussed.

II. Lorentz force in action

II.1. Practical aspects

Electromagnetism appears everywhere around us and the LF as a non-dividable part of it plays important role in many processes of macro and micro scale in nature. People try to make use of this force in their scientific and practical activities. Earth's core surface evolution and some geophysical processes can be analyzed on the basis of changes in horizontal LF acting everywhere at the core surface [2]. It is demonstrated [3] that the LF and the force of electric fields acting on charged particles that exist in atmospheric vortex phenomena plausibly contribute to the physical effects that will explain tornados and other atmospheric vortex phenomena. The possibility of raising an artificial tornado generated by LF and some other practical aspects of this problem are also discussed in [3].

Application of electromagnetic fields during structure formation in cast materials is not so largely investigated. Some of the results reported by different authors are contradictable and not well explained. There are two lines of utilization of electromagnetic forces during solidification. The first is related with influence on transport phenomena near to solid/liquid interface. Here microstructure formation and potentials for its control in various metals and alloys are the object of interest. The second line is related with manipulation of gravity effects in macro- and microstructure formation in MMCs. There are limited works devoted to melt infiltration in preforms or other porous media.

Thermoelectric effects on solid/liquid interface in solidified metallic melts are similar to Seebeck effect in a thermocouple. They account for the existence of electric microcurrents around growing dendrites. If the solidification runs in magnetic field, then LF appears in the dendritic network according to (3) and affects the process of dendrite growth. The influence of this LF on final structure is reported in a number of papers. Two alloys, Cu-60 wt. % Ag and Al-10 wt. % Cu, were investigated in [4]. It has been found that during solidification under high temperature gradient (continuous casting) the thermoelectric LF may be used either to brake or to enhance convection. This effect could then be used, for example, to increase radial segregations during solidification: the solute would accumulate in one part of the sample and the metal would be purified.

Thermoelectric convection around growing dendrites and contribution of LF to the formation of microstructure in various alloys are also experimentally and theoretically investigated in [5-10]. The influence of an axial high magnetic

field (up to 10 T) on the liquid–solid interface morphology and solid microstructure has been investigated experimentally during Bridgman growth of Al–Cu hypoeutectic alloys [5,6]. It has been found that the field causes the interface to become destabilized and irregular, and promotes planar–cellular and cellular–dendritic transformation. A brief theoretical analysis of thermoelectromagnetic convection is provided in [7,8]. To validate this analysis, the same Al–Cu hypoeutectic alloys are solidified directionally under a magnetic field, and both the interface shape and cellular morphology in the mushy zone are investigated. The same effects are reported for Zn-2 wt. % Cu alloy in high magnetic field of 12 T [9]. The effects of higher values of LF on the Al–Al₂Cu and Pb–Sn lamellar eutectics during directional solidification are investigated experimentally in [10]. The results show that the application of a strong magnetic field caused morphological instabilities and deformation of the eutectic lamellae. It has been demonstrated experimentally on the basis of Al–0.85 wt. % Cu alloy and pure Al [11] that experimental evidence exists for the formation of stress in the solid near the liquid/solid interface when relatively high values of LF are used. This stress is the reason for the interface morphological instability.

Alternatively, LF is successfully used to influence the macrosegregation in continuous casting. The results show [12] that electromagnetic casting process can effectively reduce macrosegregation, and electromagnetic frequency has a great influence on solute distribution along the radius of ingot. It is reported that for ingot of 200-mm diameter from 7075 aluminum alloy (5.70 Zn, 2.30 Mg, 1.43 Cu, 0.20 Cr, 0.20 wt. % Mn,) the frequency of 30 Hz eliminates completely macrosegregation.

In fact, the gravity affects all physical processes in a liquid. This effect can be negligible in some processes but for other it plays an essential role. For example, important phenomena caused by gravity in suspensions, colloids and pure liquids are: flotation, sedimentation, convection, phase segregation and others. Physical characteristics such as pressure, interfacial phenomena and wettability for listed substances are directly connected with the gravity. Consequently, each attempt for manipulation of the gravity will change the physical basis of the above processes and characteristics. These processes and characteristics are very important in a great number of technologies, and especially in new materials design. That is why deeper understanding and elaboration of the gravity affecting techniques can be considered a challenge in the modern engineering.

The simplest way to produce reduced or zero gravity is by use of space labs or airplanes flying on a special trajectory. The biggest disadvantage of

these two approaches is that both are costly and the second one provides weightlessness for a short period of time only.

The technique applied most often to avoid some gravity effects in the synthesis and investigation of metallic materials is electromagnetic levitation. For example, this technique has been widely used by Ivan Egry *et al.* during the last 10 years. He applied electromagnetic levitation in measurements of surface tension, viscosity, electrical conductivity and density of undercooled melts [13,14], to study short-range chemical order in various metallic liquids with compositions corresponding to intermetallic solid phases [15-17]. Very interesting results obtained for Co-Cu alloys under the levitation and microgravity (on rocket board) conditions are discussed in [18].

The kinetics of liquid-phase separation in $\text{Cu}_{50}\text{Co}_{50}$ alloys is investigated by combination of conventional electromagnetic levitation with a strong magnetic field (2T) [19]. The experiments have revealed a singular size distribution for the minor Cu-rich phase in a Co-rich matrix, which differs from a bimodal distribution under a zero field. Such an effect of the LF is similar to that of reduced gravity during parabolic flights.

The most attractive application of LF is related with manipulation of gravity effects during formation of cast composite structures, and that is exactly what we are planning to investigate in details in this project. We will focus our attention on LF that appears in electroconductive liquids, when: (i) constant direct current exists in the liquid and (ii) the liquid is subjected to constant magnetic field, whose direction does not coincide with the current.

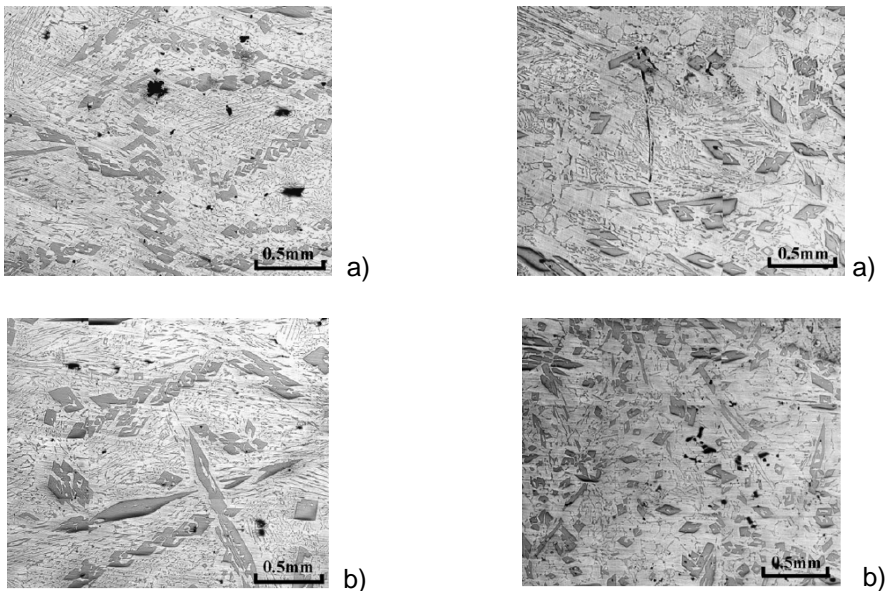
The idea of FGMs was substantially advanced in the early 1980's in Japan, where this new material concept was proposed to increase adhesion and minimize the thermal stresses in metal-ceramic composites developed for reusable rocket engines [20]. Meanwhile, FGM concepts have stimulated worldwide research activities and are applied to metals, ceramics and organic composites to generate improved components with superior physical properties [21].

Today production of FGM can be considered a next step in composite materials development. They are specific class of engineered materials in which the composition and/or microstructure varies in one specific direction by a continuous change and does not possess any specific interfaces. Therefore, it is generally assumed that such a material should better resist the thermal and mechanical cycling. The application of this concept to MMCs leads to the development of materials/components designed with the purpose of being selectively reinforced only in regions requiring increased modulus, strength and/or wear resistance. The graded structure means graded properties and

obtaining of such structure enlarges in an essential degree the range of industrial applications of the materials considered, especially of MMCs. The production of FGMs is a special process in which the gravity should be either „stimulated” or „limited”. The development of instruments for micro- and macrostructure design in FGMs is of major importance for the modern material science. It should be noted that mathematical modeling and numerical simulation are extremely helpful instruments for design and characterization of FGMs [22], which are, in fact, typical representatives of knowledge-based materials.

There are limited results on new materials formation under control by LF. Such approach has been recently used for structure control during solidification of Al and Fe alloys and MMCs reinforced by particles [23-29].

Functionally graded materials obtained by solidification of aluminum alloys in the field of Lorentz force are reported in [24]. The experiments have been carried out with Al–12 wt. % Ni, Al–17 wt. % Ni, and Al–23 wt. % Ni alloys and the distribution of a primary Al_3Ni phase in these alloys was investigated. The obtained results demonstrate that, as shown in Fig. 2, without application of the electromagnetic field, the primary phase is of an almost homogeneous distribution, whereas solidification in the field of LF results in graded distribution of the primary phase, Fig 3.



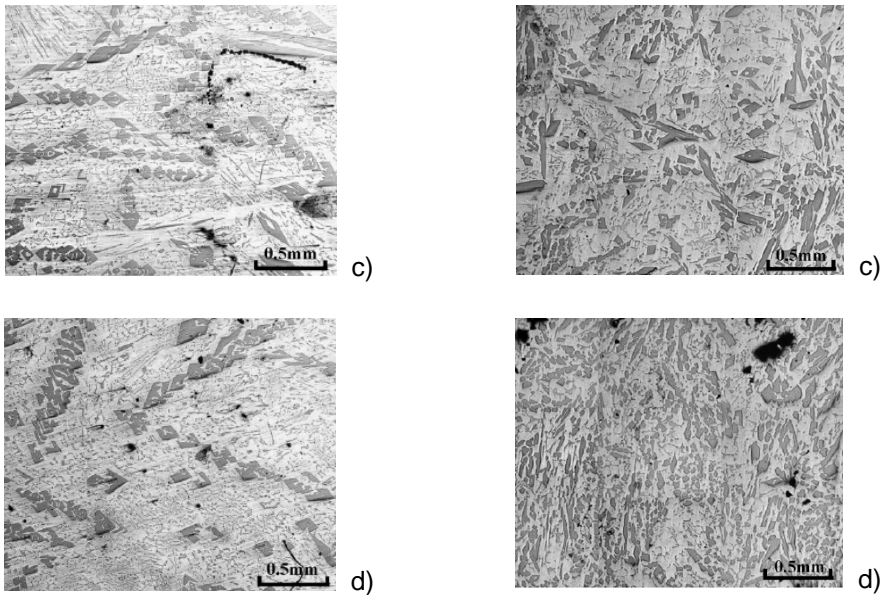


Figure 2. Distribution of Al_3Ni phase in Al-12 wt. % Ni sample without application of LF field: a), b) c) and d) are microstructures of the upper, middle and lower sample region, after [24]

Figure 3. Distribution of Al_3Ni phase in Al-12 wt. % Ni sample with application of LF field: a), b) c) and d) are microstructures of the upper, middle and lower sample region. LF is directed downward, after [24]

The formation of graded distribution of the primary Al_3Ni phase when the melt solidifies in LF field can be easily observed. The same graded distribution has been found in the other two alloys under investigation, Fig. 4.

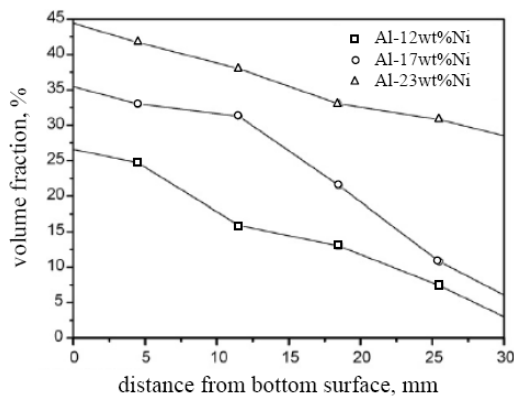


Figure 4. Distribution of volume fraction of the primary Al_3Ni phase in samples obtained after solidification of three Al-Ni alloys in LF field, after [24]

The same authors have studied the formation of graded distribution of Mg_2Si particles in Al-5 Si-4 Ti wt. % matrix [26]. Such distribution is shown in Fig. 5.

A complex investigation of relations between major processing parameters and final particle distribution is also presented.

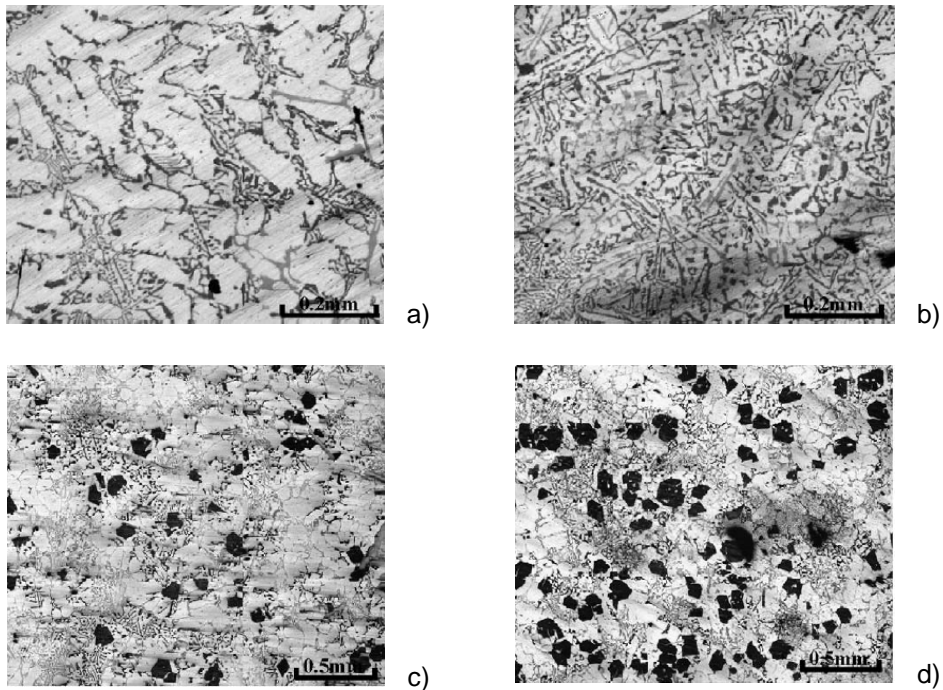


Figure 5. Microstructures of Al-5 Si-4 Ti wt. %/ Mg_2Si sample solidified in LF field: a) and b) the upper part (particle-free region), c) the transition region, d) the lower part (particle-rich region), after [26]

Solidification in electromagnetic field results in refinement of the microstructure. Lorentz force is also used as specific antigravity instrument [30] in processing of immiscible liquids, and in production of materials for self-lubricated bearings or Pb/Al plates for acid accumulators. Our preliminary experiments with particle distribution control in Al-Si/SiC_p composites have yielded very promising results [31]. The US company Elecmatec Ltd. states that it is the owner of a technology based on LF utilization, Fig. 6, which allows controlling gravity segregation during casting of metals. This technology can be used for production of metal composite materials under micro-gravity conditions, i.e. under the conditions that exist in space. It allows production of

either highly homogeneous or graded structures from alloy compositions in which more than one phase is present in the liquid state.

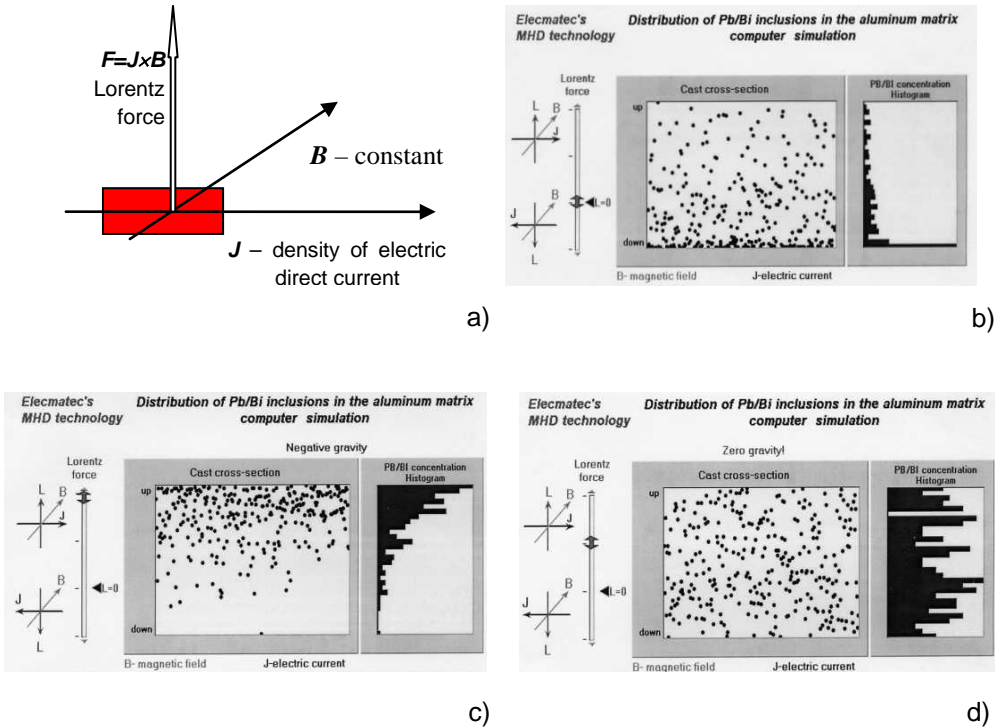


Figure 6. Effects of Lorentz force acting in MMCs suspensions: a) nature of the force applied on arbitrary volume in a melt; b) particle distribution when the force is zero; c) particle distribution when the force is opposite to gravity and overcomes it; d) particle distribution when the force is opposite to gravity and “eliminates” it (courtesy of Elecmatec Ltd.)

Elimination of gravity effects can result in important changes in some physical phenomena in suspensions. Such an example is the process of Ostwald-ripening of Cu particles in a liquid Pb-Cu melt with low volume content of the phase dispersed [32]. Providing almost zero gravity in the melt for a long time, the authors have found that the particle growth differs significantly from the growth law of the conventional theory for diffusion-controlled Ostwald ripening, indicating that in this system the particle coarsening is not only diffusion limited. To explain this phenomenon a new growth model has been developed.

Manipulation of gravity by LF can be used to separate oxides and other non-metallic inclusions from molten metal as an alternative to expensive and sometimes unreliable filtration systems. Moreover, the idea for solidification of metals, alloys and composites in electric, magnetic or electromagnetic fields can be successfully utilized as a cheaper way for purification of liquid metals, alloys and all electroconductive chemical substances. By means of LF, the secondary phases dispersed in base liquid can be moved and kept in different areas of the liquid.

Generally speaking, LF induced by simultaneous action of crossed constant magnetic and electric fields allows obtaining of not only graded but also homogeneous structures from metal melts, which consist of two or more components. One or more components of the melt can be solid as in MMCs. By efficient manipulation of the magnitude and direction of the electric and magnetic fields it is possible to obtain various distributions of reinforcing particles in the metal matrix. The same particles can be settled at the top or at the bottom, or can be homogeneously distributed in the solidified ingot. There are some mandatory requirements, which must be satisfied to make use of LF. First of all, the base liquid must be electrically conductive, which is valid for all metal melts and many other liquids. The second requirement follows from equation (6). According to this equation, for Archimedes force to appear in the Lorentz field, the electrical conductivity of the dispersed phase and base liquid must be different. Obviously, the third requirement is the mold to allow penetration of magnetic field. The dispersed phases in the base liquid can be solid, immiscible liquid, or even gaseous as the phases divided on solid/liquid interface during solidification. Lorentz force can be successfully used for purification of liquids, for removal of different inclusions, for process control and for other applications.

There are some important limits of this approach determined by the physical nature of the Lorentz field. First of them follows from (3)-(5). Each inhomogeneity in source fields (electric and/or magnetic) results directly in inhomogeneity of the Lorentz field. This, in turn, generates pressure inhomogeneity in the base electroconductive liquid and consequent local fluid flows. Such inhomogeneity can be caused by a specific geometry of the vessel (mold) containing the base liquid, by thermal convection and by other phenomena. As a result, the process of additional mixing will start in the liquid, generating free surface instability. The latter usually increases the non-homogeneity in the source fields. To avoid such effects in liquid composite melts, if mixing during solidification is to be suppressed, closed molds (without free surfaces) and molds with strongly parallel inner surfaces are recommended for use.

II.2. Mathematical description of main physical processes during solidification in LF field

Numerical simulations in cast practice are being extensively used to improve technology, to optimize design, to increase cast products quality and very often to elaborate new materials. All simulations are based on more or less detailed mathematical description of physical phenomena involved in the process of final product formation. The complex of physical phenomena related with structure formation of particulate reinforced MMCs during their solidification in the field of LF consists of:

- Thermal processes – heat transfer and phase changes due to cooling of casting-mold system;
- Movement of the reinforcing phase due to gravity, LF and mixing caused by electromagnetic forces;
- Mechanical processes – development of thermal stresses inside the solidified area and shrinkage due to the deformability of the solidified shell in the mold;
- Magnetohydrodynamic processes:
 - electromagnetic phenomena related with penetration of the magnetic field in the melt, which together with electric current determine the existence of LF in a liquid part of the solidifying volume;
 - hydrodynamic phenomena determined by natural convection due to the gradient of temperature (gravity effect) and by Lorentz field in the liquid phase.

All these processes are deeply related to the physical properties of the materials. These properties also vary with time because of phase changes (solidification of melt) and changes of composition due to movement of the reinforcing particles. Moreover, the processes of different types influence each other. For example, variation of the particle percentage in certain volume of the melt changes the current density in this volume which, in turn, changes LF. Variation of LF generates different conditions for the fluid movement and consequently for the heat transfer in the volume considered. Because of this, all the above mentioned processes should be considered in their interconnectivity.

II.2.1. Heat transfer and phase change

In the experiments considered here, the solidification of composite melt takes place in a ceramic mold, as shown in Fig. 7. The ceramic mold is closed and is specially designed for this technology. The graphite electrodes are fixed permanently to the mold walls. The volume filled by the liquid is of a $l \times w \times h$ size. All physical properties (thermal conductivity, density, specific thermal capacity) of the composite are calculated by the rule of mixture. For the sake of simplicity, the computational domain can be regarded as a region occupied by the composite melt. The origin of the coordinate

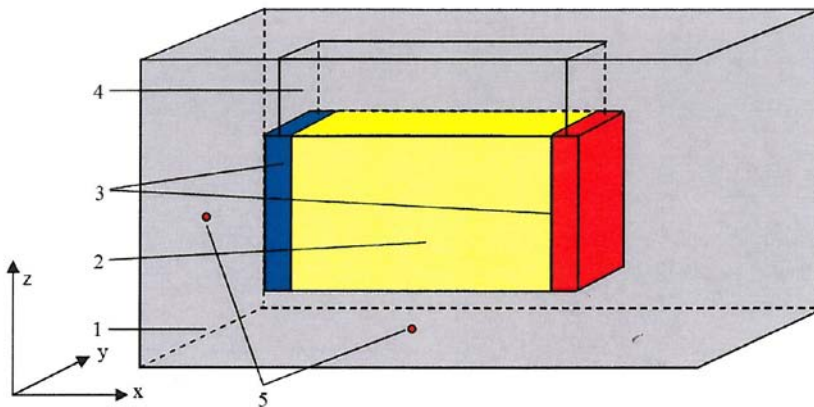


Figure 7. Principle chart of experimental mold (cross-section): 1 – ceramic mold; 2 – composite melt; 3 – graphite electrodes; 4 – ceramic mold cover; 5 – thermocouples

system is placed at the center of the bottom surface of the computational domain. In experiments, the thermal conditions on the lower and upper mold surfaces are different and symmetry exists only in the 'x' and 'y' directions but not in the 'z' direction. Because of this, only one quarter of the computational domain can be considered. In such a case the temperature field $T(x,y,z,t)$ obeys the equation

$$\rho C_{\text{eff}} \frac{\partial T}{\partial t} = \text{div}(\lambda \text{grad}T), \quad t > 0, \quad x \in (0, l/2), \quad y \in (0, w/2), \quad z \in (0, h), \quad (13)$$

where

$$C_{eff} = (C_p + L \frac{\partial f_L}{\partial T}) \quad (14)$$

Here the thermal conductivity depends on temperature and percentage of the reinforcing phase, $\lambda = \lambda(T, c_p)$.

The dependence of the liquid fraction f_L in the mushy zone can be expressed by linear form. In this case the derivative is expressed as:

$$\frac{\partial f_L}{\partial T} = \begin{cases} 0 & \text{for } T < T_S \\ \frac{1}{T_L - T_S} & \text{for } T_S \leq T \leq T_L \\ 0 & \text{for } T > T_L \end{cases} \quad (15)$$

For eutectic composition, the solidification occurs at the eutectic temperature $T_{cr} = T_L = T_S$. Then, to provide stability of the numerical algorithm for solution of (13), it is assumed that phase transformation is in progress within a narrow temperature interval: $T_L = T_{cr} + 1$ and $T_S = T_{cr} - 1$.

The initial condition is expressed by a uniform temperature in the computational domain at time $t = 0$.

On the symmetry planes we impose the usual symmetry conditions:

$$\frac{\partial T}{\partial x}(0, y, z, t) = 0, \quad 0 < y < w/2, \quad 0 < z < h/2, \quad t > 0 \quad (16)$$

$$\frac{\partial T}{\partial y}(x, 0, z, t) = 0, \quad 0 < x < l/2, \quad 0 < z < h/2, \quad t > 0$$

We assume that heat transfer on the lower and upper surfaces is defined by relations:

$$\frac{\partial T}{\partial x}(x, y, 0, t) = \alpha_1(T(x, y, 0, t) - T_1), \quad 0 < x < l/2, \quad 0 < y < w/2, \quad t > 0 \quad (17)$$

$$\frac{\partial T}{\partial x}(x, y, h/2, t) = \alpha_2(T(x, y, h/2, t) - T_2), \quad 0 < x < l/2, \quad 0 < y < w/2, \quad t > 0$$

Here T_1 and T_2 are the average temperature of the lower and upper part of the ceramic mold, respectively, and α_1 and α_2 are the relevant heat exchange coefficients.

On the lateral surfaces, at $x = l/2$ (contact with the graphite electrode) and $y = w/2$, the heat transfer is described by analogy

$$\frac{\partial T}{\partial x}(l/2, y, z, t) = \alpha_3(T(l/2, y, z, t) - T_3), \quad 0 < y < w/2, \quad 0 < z < h, \quad t > 0 \quad (18)$$

$$\frac{\partial T}{\partial x}(x, w/2, z, t) = \alpha_4(T(x, w/2, z, t) - T_4), \quad 0 < x < l/2, \quad 0 < z < h, \quad t > 0$$

Here T_3 and T_4 are the average temperature of the graphite electrode and of the lateral part of the ceramic mold, respectively, and α_3 and α_4 are the relevant heat exchange coefficients.

The equations (13)-(18) define the temperature in the solidifying composite ingot. Let us recall that the thermal conductivity λ depends substantially on the local concentration of the reinforcing phase.

II.2.2. Dynamics of reinforcing phase concentration

The movement of reinforcing particles during the composite melt solidification is one of the key phenomena in the technology considered here. The control of particle distribution during melt solidification is of major importance for obtaining of particulate reinforced MMCs with graded structure and properties. Therefore, special attention should be devoted to a very precise description of this phenomenon.

One of the forces determining the single particle movement in a liquid is the drag force, often called Stokes' force. This force is proportional to dynamic viscosity η_0 of the liquid. For spherical particles, the drag force is expressed by the last formula in Table 1. The case of multiparticle movement differs from single particle movement because of number of reasons. Stokes' law gives very simple expression for the drag force and it is quite often used for a quantitative assessment of various physical processes. In the case of processes characterized by multiparticle movement in liquid, this law must be modified. The modification consists in introduction of apparent viscosity (related to suspensions) instead of simple viscosity (related to pure liquid). For the purposes considered here, it is recommended to use the following formula [33] for apparent viscosity, which is in conformity with the particle volume fraction

$$\eta = \eta_0(1 + 18.5V_f + 4.5V_f^2 + 170V_f^3) \quad (19)$$

To express the drag force applied to a single particle which moves in multiparticle suspension, we can apply again the conventional formula for Stokes' law with apparent viscosity given by (19) instead of dynamic viscosity η_0 , i.e.:

$$\mathbf{F}_S = -6\pi\eta r_0 \mathbf{v} \quad (20)$$

Now equation (6) with \mathbf{F}_S defined by (20) determines the trajectory of a single particle in suspension. An effective algorithm for calculation of the dynamics of particle volume fraction on the basis of single particle movement is discussed in [33]. Details for numerical solving of this problem can be found in [34, 35].

II.2.3. Mechanical processes

The mechanical processes taking place in a solid body are determined by the thermo-elasto-plastic state of this body. These processes determine in an essential degree the defects and mechanical properties of cast products. Nevertheless, as they have relatively small impact on final reinforcing particle distribution, they will be not in the focus of our interest. Explicit equations and methods for numerical solving of such a problem are discussed in details in [36,37].

II.2.4. Magnetohydrodynamic processes

Here, equations related with the magnetohydrodynamic processes in the solidifying melt will be given. Let us consider a region with the metallic melt solidifying in constant electric and magnetic fields. In this case, the joined magnetohydrodynamic system looks as follows:

- Maxwell's equations

$$\operatorname{rot} \mathbf{B} = \mu \mathbf{j} \quad (21)$$

$$\operatorname{rot} \mathbf{E} = 0 \quad (22)$$

$$\operatorname{div} \mathbf{B} = 0 \quad (23)$$

- generalized Ohm's law

$$\mathbf{j} = \sigma (\mathbf{E} + \mathbf{v} \times \mathbf{B}) \quad (24)$$

- hydrodynamic equations

continuity law

$$\operatorname{div} \mathbf{v} = 0 \quad (25)$$

and Navier-Stokes's equation

$$\rho \left(\frac{\partial}{\partial t} \mathbf{v} + \mathbf{v} \cdot \operatorname{grad} \mathbf{v} \right) = \eta \Delta \mathbf{v} + \operatorname{grad} p + \rho \mathbf{g} + \mathbf{f}^L \quad (26)$$

where the density of LF is expressed by

$$\mathbf{f}^L = \mathbf{j} \times \mathbf{B} \quad (27)$$

The current density \mathbf{j} is provided by the Maxwell's equations presented above.

The system of equations (21)-(27) describes magnetohydrodynamic phenomena in the solidifying metallic melt displaced in constant magnetic and electric fields. These equations, together with the equations describing heat transfer, the dynamics of reinforcing particle concentration, the evolution of thermal stresses and appropriate boundary conditions, form a complex model of the basic physical phenomena involved in casting under here discussed LF.

When the shape of the ingot is simple as the one shown in Fig. 7, there is no need for the Maxwell's equations (21)-(23) to be solved. In this situation, the electric field strength \mathbf{E} can be considered constant over the entire ingot volume. For calculation of the current density in (27) only formula (24) can be used, but the specific electrical conductivity σ should be replaced with an effective electrical conductivity obtained by the rule of mixture as follows:

$$\sigma_{eff} = \sigma(1-V_f) + \sigma_P V_f \quad (28)$$

In this way, the LF term in the Navier-Stokes's equation (26) is expressed by relation

$$\mathbf{f}^L = \sigma_{eff} (\mathbf{E} + \mathbf{v} \times \mathbf{B}) \times \mathbf{B} \quad (29)$$

If fluid velocity is small enough to be neglected, the last equation is transformed into

$$\mathbf{f}^L = \sigma_{eff} \mathbf{E} \times \mathbf{B} \quad (30)$$

For specific practical applications it is very interesting to obtain ingots of sophisticated geometry. Such cases are briefly discussed under section IV.2. below. In this situation \mathbf{E} is not constant in the ingot volume any longer and formulae (28)-(30) cannot be used directly. The current density in (27) can be determined by the solution of Maxwell's equations (21)-(23). Here some difficulties arise with the determination of boundary conditions, which are specific for each particular geometry. Details of such a model can be found in [38].

III. Project aim, objectives and activities

Irrespective of various investigations related with LF effects in electroconductive liquids, suspensions and emulsions, the results are very far from effective industrial application. Scientists and engineers are only at the beginning of the large theoretical and experimental investigations and good results, especially for graded cast materials, are yet to be obtained.

III.1. Aim and tasks

The main aim of the project proposed is to develop effective instruments for manipulation of the gravity effects in suspensions, emulsions and pure liquids. The major efforts will be directed to elaboration of technological basis for production of new FGMs.

Within the frame of this project we will investigate possibilities for obtaining some FGMs with special applications and technologies for *in-situ*

control of graded or homogeneously structured MMCs. Additionally, various techniques for phase separation, purification and homogenization of multiphase liquids will be tested. Due to the small number of experimental and theoretical studies for control of the gravity effects by LF there is little prospect of obtaining some unexpected results with important practical applications.

The **objectives** of this project can be summarized as follows:

1. To elaborate effective instruments for manipulation of gravity effects in metallic suspensions by means of Lorentz force;
2. To establish processing conditions for *in-situ* micro- and macro-structure control of some FGMs. To obtain some MMCs of the graded structure and properties;
3. To study possibilities for improving the mechanical properties of materials obtained by additional mechanical processing (rolling and forging);
4. To find effective methods for phase separation of components in electroconductive suspensions and colloids;
5. To determine numerous qualitative and quantitative relations between processing parameters and final composite structure;
6. To elaborate mathematical model for the complex of physical processes that take part in the graded structure formation.

The **tasks** that must be solved for the project realization are as follows:

1. To find processing conditions for the formation of graded metallic composites with aluminum alloy matrix and SiC_p particles as a reinforcing phase by varying magnitude of LF.
2. To study main structure characteristics and mechanical properties of the materials obtained.
3. To describe quantitative relations between the intensity of the Lorentz field and the structure and properties of the materials.

Numerous samples will be also prepared from the obtained materials and will be delivered to the Institute of Metal Science in Sofia for additional mechanical processing (rolling and forging) to improve further their structure and mechanical properties.

III.2. Activities

The activities under this project are directly related with the tasks that must be fulfilled. Numerous experiments will be carried out on real composite materials and basic structure characteristics of the obtained materials will be also investigated.

Various instruments for control of the graded structure formation will be tested.

III.2.1. Experiments with real MMCs

The experimental work is related with studies of the graded structure formed in real MMCs with particles as a reinforcing phase. Aluminum/silicon alloys will be used as a composite matrix and SiC particles as a reinforcing phase.

III.2.2. Structure investigations

The distribution of particles in the fabricated composites will be examined. The obtained structure will be investigated by light microscopy, scanning electron microscopy and transmission electron microscopy (SEM and TEM), and by X-ray diffractometry. The investigations will be focused on macro- and microstructures of graded MMCs produced under different technological conditions. The relations between the processing parameters and the final structures obtained will be analyzed. Based on these relations, some rules for the structure management will be defined.

III.2.3. Preparation of samples for plastic processing

Samples of the materials obtained will be prepared for plastic processing at the Institute of Metal Science in Sofia. These samples will be delivered to the Institute in the course of project execution.

IV. Methodology, equipment and experiments

The project activities will run in two parallel lines: experimental and theoretical. The experimental work forms the largest part of this project. The equipment needed is a unique one and must be designed for the specific aims of the project. Obviously, the most important part of this equipment is the magnetic system. This system must meet some strict requirements such as a high value of the magnetic field intensity and the highest possible homogeneity of this field in the volume of the liquid investigated. For experiments with some model liquids (see below) we can use low intensity field generated in the inner area of a solenoid but for high intensity magnetic field, concentrators of special geometry should be designed.

As a first step, various experiments with model liquids will be carried out. Various electroconductive liquids at room temperature will be used as model base liquids. Such experiments will be used to establish some basic relations between the processing parameters, the geometry of the vessel (mold) and local particle distribution, and to outline potential applications of the technique considered. The main advantages of the model liquids are: the possibility of processing at room temperature; easy to observe major phase movements; reusable elements, and experiments continued as long as needed. Model suspensions can be mixtures of CuSO_4 water solution and small rubber pieces, or mixtures of AgNO_3 water solution and sulfur crystals. Using the immiscible liquids as stated above, the wettability under apparent super gravity or apparent microgravity will be also studied. The apparent supergravity means higher pressure in the liquid compared with the pressure at normal gravity. This gives good opportunity to study the contact angle dependence on pressure. The latter one will be controlled by LF. Most of the scientists working in this area believe that pressure does not affect in any degree the contact angle. According to the theory this is not true and the described experiments will be exceptionally useful to prove this theory. We believe that this will be a unique experimental work with an important outcome for both the theory and practice.

According to the preliminary plan, investigations will be carried out on real MMCs based on aluminum and copper alloys as a matrix and SiC_p particles as a reinforcing phase.

Very important and not so simple work is the production of disposable closed molds. Predominantly, ceramic molds will be worked out but limited quantity of quartz molds will be also made. Implantation of copper or graphite electrodes in molds needs special attention and elaboration of new practical skills. All these activities will contribute essentially to the sum of consumables.

Another component of this sum is related with expenses for chemical substances, Al and Cu alloys, composites, reinforcing phases and others.

IV.1. Equipment design and preliminary experiments conducted in FRI

The experimental work represents the largest part of this project. The equipment needed is a unique one and must be designed for the specific aims of the project. Obviously, the most important part of this equipment is the magnetic system. This system must meet some strict requirements such as a high value of the magnetic field intensity and the highest possible homogeneity of this field in the volume of the liquid investigated. Because of this, a collaboration with highly experienced specialists in magnetic systems is of major importance. To meet the requirements related with the experimental work and to accumulate the experience in different situations, three types of magnetic systems are made in FRI. Below their parameters will be briefly described.

IV.1.1. Electromagnet with air core

Such approach to the generation of magnetic field is very simple but allows obtaining a homogeneous magnetic field in a relatively large space. The benefit of the solenoid with air core is simple possibility to conduct principal experiments with model liquids and suspensions, and to establish some basic relationships. The main disadvantage of this approach is a technical limit in the magnitude of the magnetic field intensity that can be obtained.

A view of the electromagnet is given in Fig. 8. A transparent vessel is placed in the middle area because the magnetic field here is of the highest value and is homogeneous. This vessel is used for experiments with model liquids at room temperature. To estimate the intensity of the magnetic field and its homogeneity, a number of calculations by special software have been done. The results are shown in Fig. 9. The results indicate that the magnetic field in the middle area is characterized by high degree of homogeneity (constant value in a relatively large area) for distances between the two coils at intervals of 0.04m – 0.08m. It has been chosen to operate at a distance of 0.04m because there is enough room for the experimental vessel. In this case the intensity of the magnetic field is 0.048 T. The magnetic field homogeneity is also acceptable in 0.1m×0.1m area of the middle part between the coils, see Fig. 9 c) and d), which offers the work space sufficiently large for our purposes.

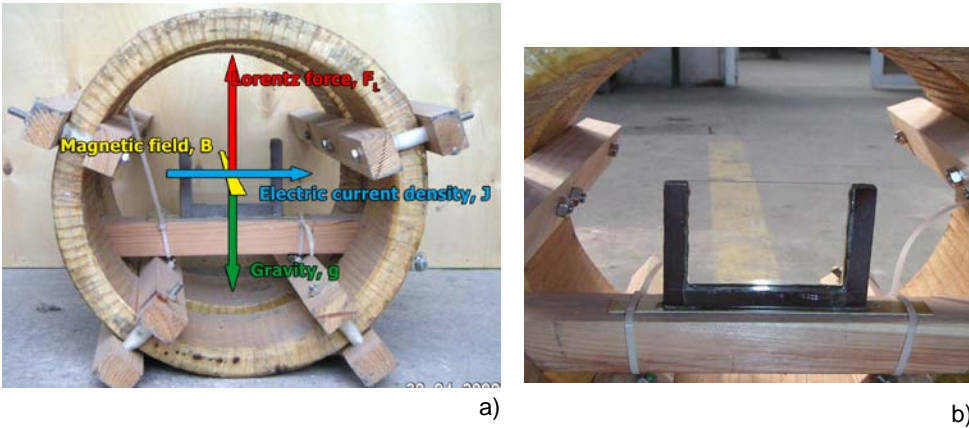


Figure 8. Electromagnet with air core: a) front view with transparent vessel in the middle part and a scheme of the applied field; b) vessel situated between the two coils (courtesy of FRI)

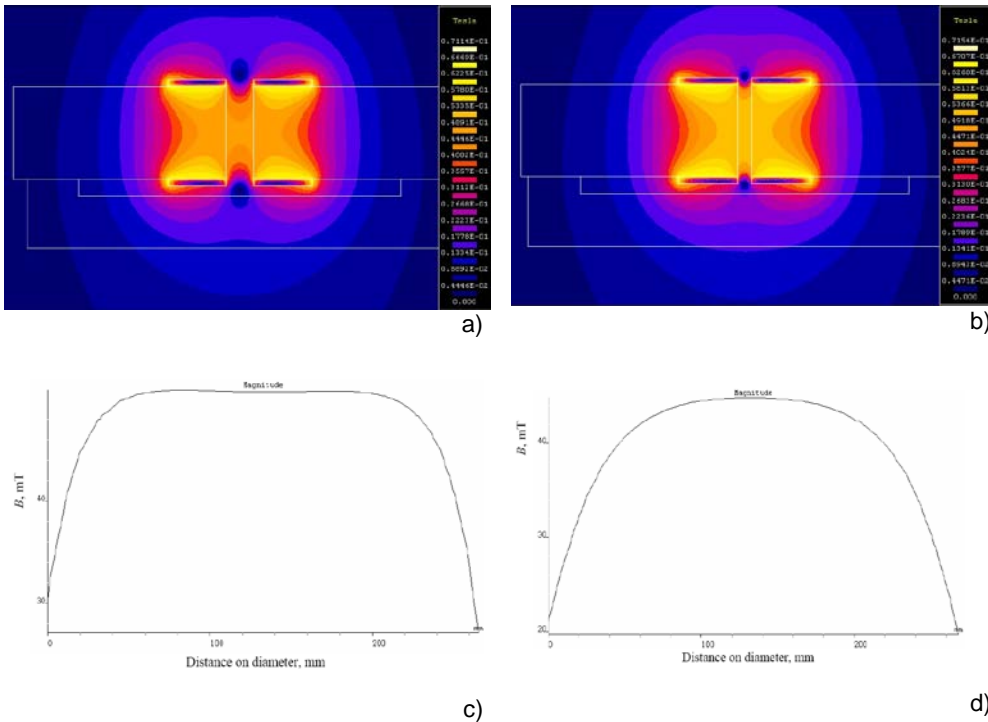


Figure 9. Calculated magnetic intensity B of electromagnet with air core: a), b) color diagrams for 0.04 m and 0.08 m spacing between the coils, respectively; c), d) values in cross-section between the coils for 0.04 m and 0.08 m spacing, respectively. The calculations were provided by MAGNETO Company Częstochowa

IV.1.2. Constant magnet

Another option to provide a magnetic field is constant magnet. Such magnet can generate stronger magnetic field than the electromagnet with air core but its operating space is smaller. Nevertheless, it is very suitable for experiments with model suspensions and some metallic composites. The constant magnet shown in Fig. 10 is used in the experiments with metal composite DURALCAN (AlSi7Mg/20 vol.% SiC_p).

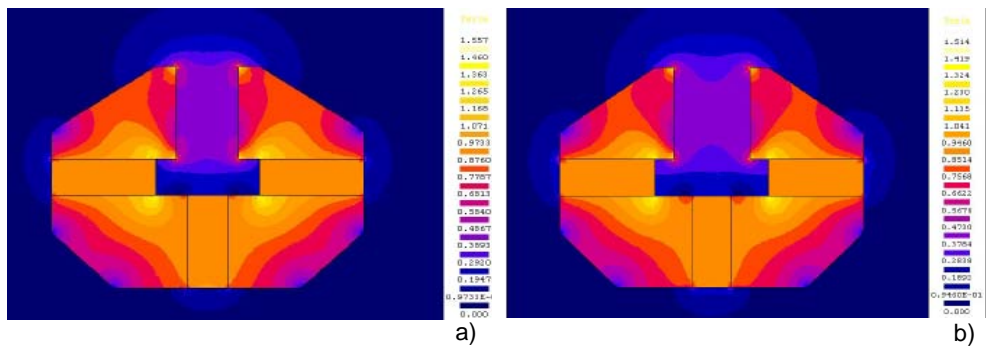


Figure 10. View of the constant magnet used in experiments. The operating space is 0.10×0.05×0.04 m (courtesy of FRI)

The intensity B of the magnetic field in the air gap between the poles is calculated for various distances. Information on the field homogeneity in a central flat between the poles is also obtained. The results are shown in Fig. 11. It can be seen that the field here is 10 to 20 times stronger than in the previous case. The field remains homogeneous over a very large area which creates good opportunity for use of a relatively large work space. In the experiments described below, the distance between the poles is 0.04m which provides $B = 0.4\text{T}$ in the work space. This magnet is easy portable, there is no need of electrical source and it can be successfully used in experiments with liquid metals.

IV.1.3. Electromagnet with high-magnetic conductivity core

To provide more flexible conditions for work not only with model suspensions and some metallic composites but also with a large class of alloys and particulate reinforced MMCs, a third magnetic system has been designed and produced. The magnetic core is made from ARMCO-Fe. This system generates magnetic fields of the highest intensity B . The electric current is supplied by high-power accumulators. Principal chart of the magnetic core is shown in Fig. 12 a). The mass of the core is about 800 kg. A view of the real electromagnet can be seen in Fig. 12 b). Preliminary calculations show that the maximum intensity of the magnetic field obtained with this electromagnet is 1.1T. In this case the magnetic field is in fact constant in a coaxial 0.20 m diameter cylinder between the magnet poles. All these parameters are obtained with a 0.08 m space between the poles, which provides large enough operating space. In future, by means of small changes in the design, the magnetic field of a $B \sim 2T$ intensity can be obtained. This will enlarge the potential of using an electromagnetic system for the flexible control of gravity effects during structure formation in particulate reinforced MMCs.



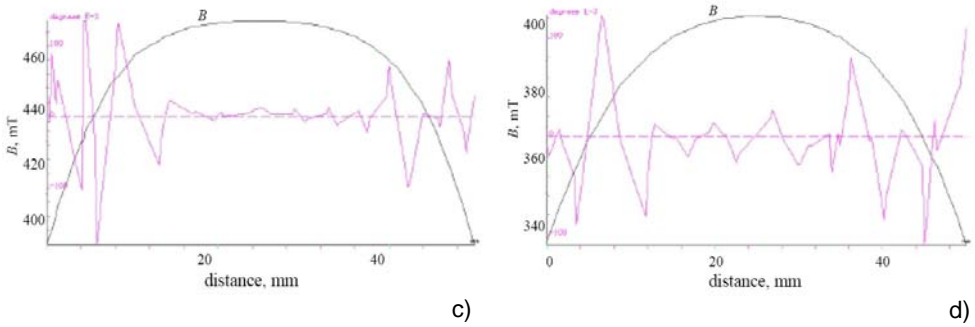


Figure 11. Calculated magnetic intensity B of the constant magnet: a), b) color diagrams for 0.03 m and 0.04 m spacing between poles, respectively; c), d) values in cross-section between the poles for a 0.03 m and 0.04 m spacing, respectively. The calculations were provided by MAGNETO Company Częstochowa

The same system will be successfully used in experiments with manipulation of gravity effects in various electroconductive suspensions and emulsions.

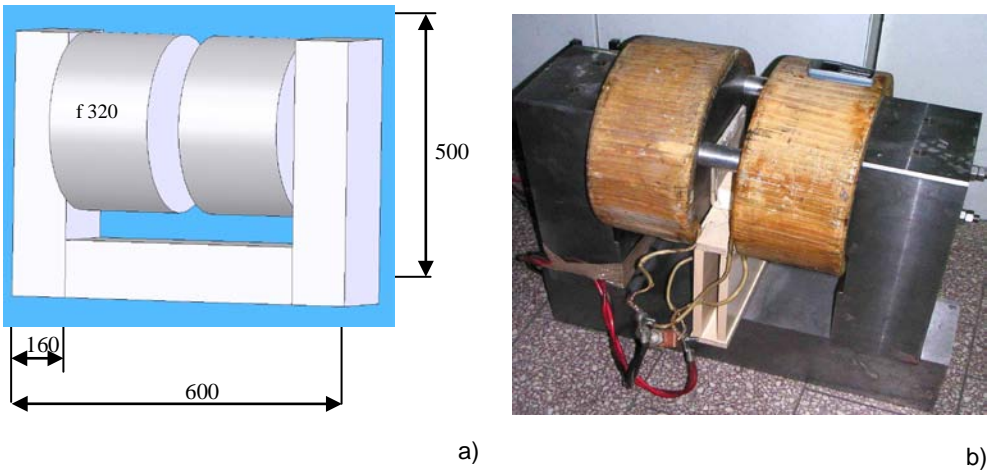


Figure 12. Electromagnet with high-magnetic conductivity core: a) principal chart and dimensions; b) general view

IV.1.4. Experiments with model liquids

The model liquids are transparent electroconductive water solutions of various chemical substances. The aim of such experiments is to test the equipment and to find limits of its applicability. They are also used to observe movement of different phases in a suspension in the gravity and LF fields, to establish some basic relations and outline further potential applications of the technique considered.

These experiments are conducted with relatively large particles of substances insoluble in the base liquid (the electroconductive water solution). Here the Lorentz field intensity is directed opposite to gravity. Thus, conditions of apparent microgravity are created. The transparent vessel is placed in constant magnetic field generated by electromagnet with air core or by permanent magnet. The current density is between 300 A/m^2 and 1400 A/m^2 .

The experiment shown in Fig. 13 demonstrates movement of rubber particles of about $3 \times 4 \times 5 \text{ mm}$ size in a CuSO_4 water solution of the density of 1100 kg/m^3 . The density of the particles is the same. The magnetic field is generated by the electromagnet with air core. At the beginning, the current density is zero (no electric field applied), Fig. 13 a). Due to the equal density of the particles and the solution, a free motion of the rubber particles in the entire liquid volume can be observed. When the electric current is switched on, the apparent microgravity conditions are generated in the base liquid and particles start moving downward in a sedimentation process, Fig. 13 b). With the electric current switched off, the particles again start floating free in the liquid.

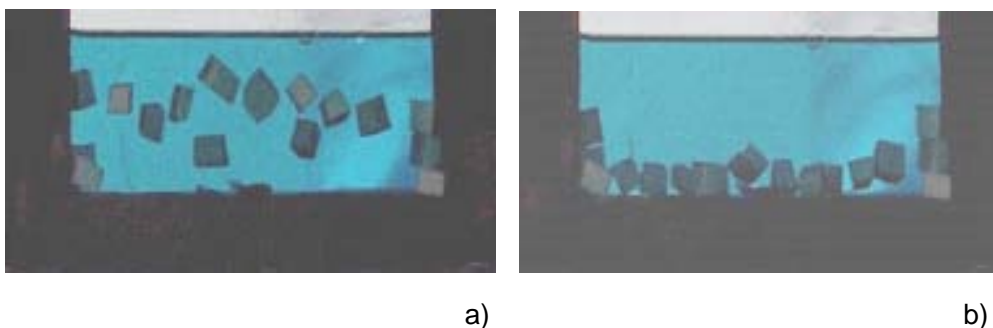


Figure 13. Movement of rubber particles in electroconductive liquid: a) the state of gravity only; b) after generation of LF field (unpublished results)

Here, because of a low intensity of the magnetic field ($B \sim 40 \text{ mT}$), the particles move slowly and the density of the particles and of the base liquid must be approximately equal.

The same experiment has been repeated in a stronger magnetic field ($B \sim 400$ mT) generated by the permanent magnet. Higher values of the magnetic field intensity allow observing the apparent microgravity effects in suspension with greater difference between the density of the base liquid and particles. Such suspension is prepared from a water solution of the 1300 kg/m^3 density obtained due to a higher content of CuSO_4 and rubber particles of 1 mm^3 volume. In absence of the electric field in a model suspension, the particles are displaced in the upper zone of the liquid, Fig. 14 a). As the electric field is switched on, the current density is established at 300 A/m^2 and the rubber particles start to redistribute at the bottom. In this case, the apparent microgravity conditions are created in the base liquid, which becomes "lighter" and the rubber particles start moving downward in an induced settling process. The Lorentz field does not act directly on the particles because they are not electroconductive. In Figs. 14 b)-f) the evolution of the settling process is shown. The particles present at the liquid/air interface (at the very upper surface of the liquid) are subjected to "end-effects" due to surface tension, and they stay motionless during the settling process. The use of stronger magnetic field in this experiment allows us to overcome the gravitational Archimedes force in the case of larger differences in the density of the base liquid and solid particles introduced into it, which means that the larger is the difference between the densities of the phases in suspension, the stronger magnetic field is needed for the manipulation of gravity effects. Experience shows that increasing of electric current stimulates mixing, which suppresses settling and flotation. It can be concluded that increasing the magnetic field intensity B instead of electric current density is a preferable way to increase LF in suspensions and colloids.

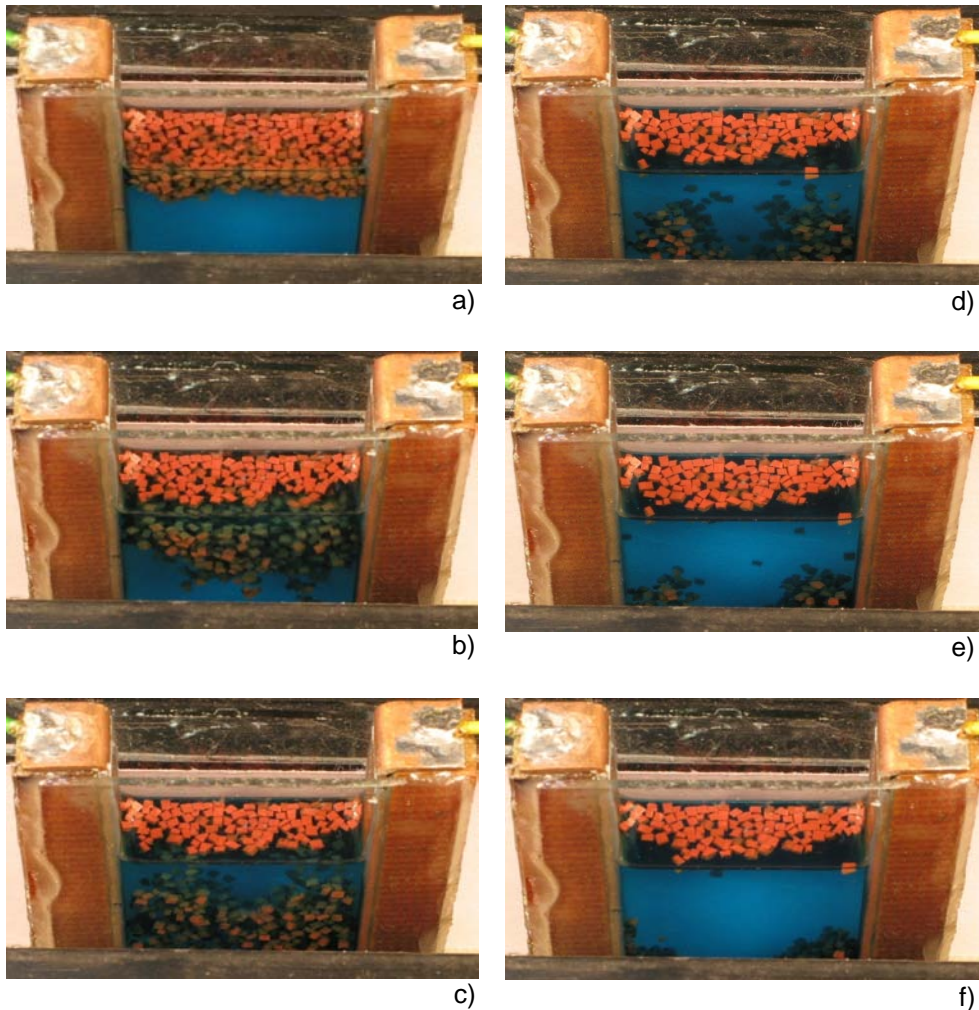


Figure 14. Induced settling process under apparent microgravity conditions in suspension of CuSO_4 water solution and rubber particles: a) starting position, $f^L = 0$; b) beginning of the process, 1s after generation of LF; c) after 2s; d) after 3s; e) after 4s; f) after 5s [31]

The induced fluid flow in base liquid (thermal convection, electromagnetic mixing) disturbs the processes of sedimentation and flotation. To avoid mixing in liquid phase, a high degree of the magnetic field homogeneity must be used. On the other hand, the generation of eddy flow in a suspension can suppress the sedimentation and flotation and provide a homogeneous dispersion of different phases. The same system as described above and shown in Fig. 14 is used to demonstrate the possibility of vortical mixing. The vessel with the suspension is placed at the end of a permanent

magnet so that the right half of the vessel is out of the work space, see Fig. 15. Such configuration generates clockwise vortex in the liquid which involves all solid particles. Simple change of the electric field polarity reverts the vortex. This experiment demonstrates the ability of LF to be used for stirring and homogenization of liquid solutions including metallic melts.

Experiments with AgNO_3 water solution of the 1600 kg/m^3 density and sulfur crystals are also conducted. To provide the same conditions for induced sedimentation, the electric current must be increased because real density of the base liquid (the water solution) is higher compared with the previous cases. Here the current density is 1400 A/m^2 . Under these conditions, the settling process of the sulfur crystals starts immediately and is completed after 3 seconds. The evolution of the process is shown in Fig. 16. The sulfur crystals that are resting at the liquid/air interface (at the very upper surface of the liquid) are subjected to “end-effects” due to surface tension and stay motionless during the settling process.

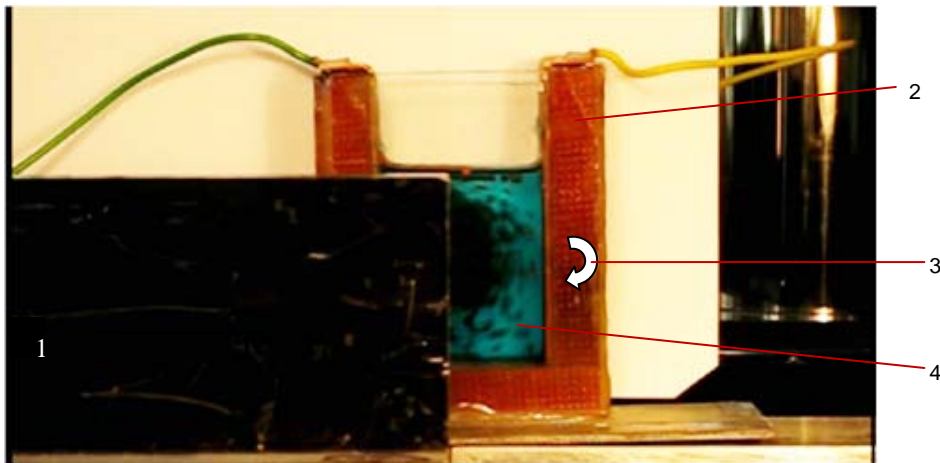


Figure 15. Generation of vertical flow in suspension: 1 – permanent magnet; 2 – transparent vessel; 3 – vortex direction; 4 – suspension (unpublished data)

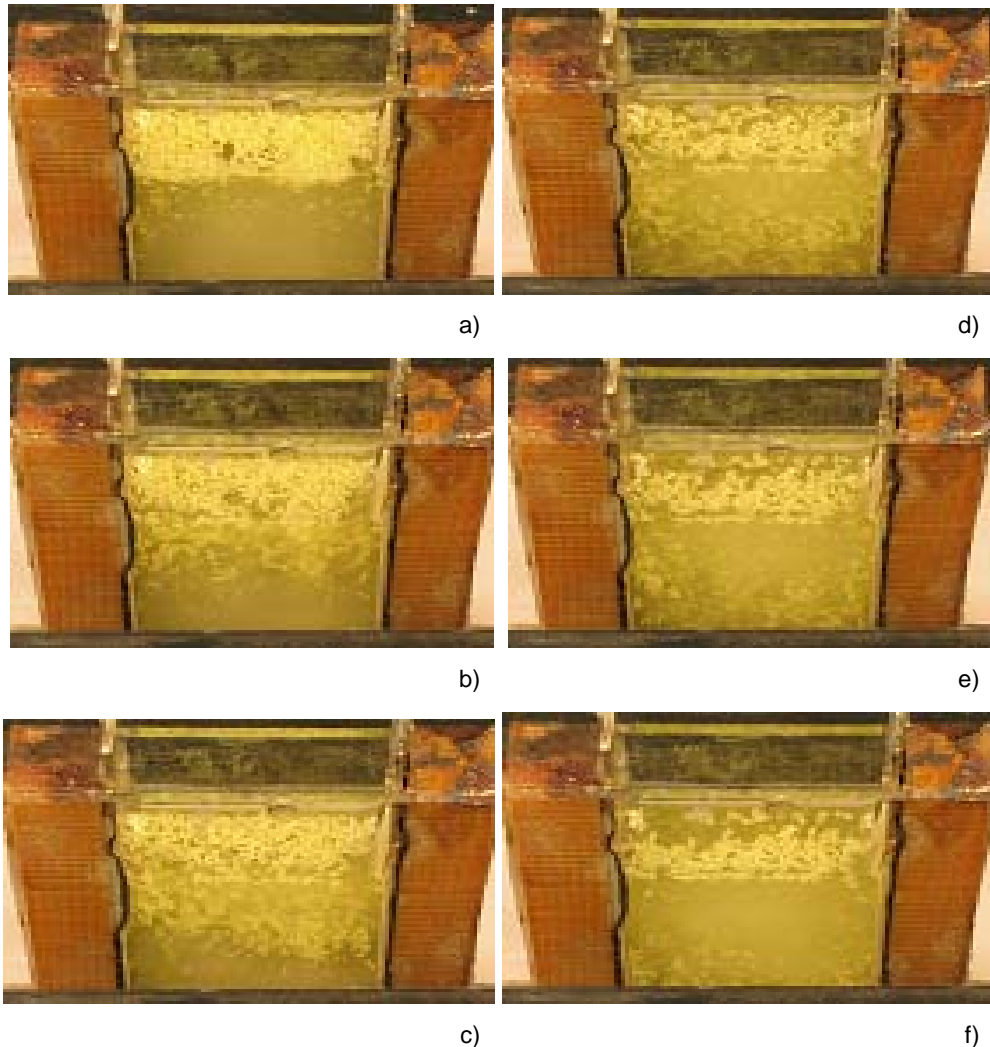


Figure 16. Induced settling process under apparent microgravity conditions in suspension of AgNO_3 water solution and sulfur crystals: a) starting position, $t^L = 0$; b) beginning of the process, 1s after generation of LF; c) after 1.5s; d) after 2s; e) after 2.5s; f) after 3s [39]

The field of LF can also be used for manipulation of gravity effects in suspension of immiscible liquids. A mixture of water solution of AgNO_3 as base liquid and CCl_4 (tetrachloromethane) as a “contamination” are used to prove such possibility. Both liquids are of a density of about 1600 kg/m^3 . Tetrachloromethane is poured into the water solution of AgNO_3 to simulate contamination of the liquid. Initially, a large drop of CCl_4 is formed in the upper region of the water solution, Fig. 17 a). After switching the electric current on, this drop is settled on the bottom of the vessel, Fig. 17 b). In this experiment,

the current density is $j = 1000 \text{ A/m}^2$ and $B = 0.4\text{T}$. The experiment is very important because it demonstrates two areas for LF applications: 1. purification (separation) of immiscible liquids; and 2. investigation of wettability under apparent supergravity or microgravity. The last option needs special attention in future studies.

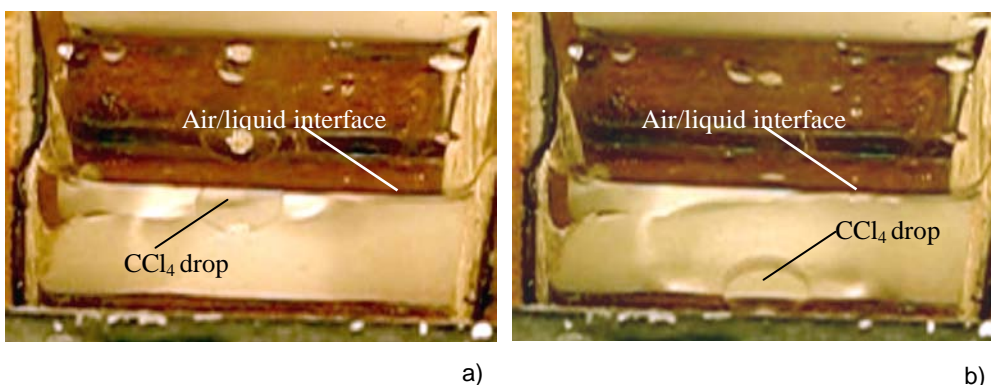


Figure 17. Induced sedimentation for immiscible liquids: water solution of AgNO_3 and CCl_4 : a) initial position of CCl_4 drop, Lorentz force is not applied; b) drop settled in Lorentz field [39]

IV.1.5. Experiments with metallic composite

Metal matrix composite of aluminum alloy AlSi7Mg and 10 vol.% SiC particles (F3S.10S) is used in experiments with metallic melt. The homogeneous magnetic field is induced by permanent magnet. The intensity of magnetic field is 0.3 T in all experiments but current density is different providing various magnitudes of LF. A ceramic mold of 0.12 m length, 0.09 m height and 0.02 m thickness is used. The ingots obtained are of a $0.10 \times 0.06 \times 0.01 \text{ m}$.

In these experiments, the F3S.10S composite solidifies in gravitational field and also under combined effects of gravity and LF (two different values of intensity B), see Table 2. The pouring temperature is 780°C . For the experiment No. 2, the electric current density is 320 kA/m^2 generating LF of the density 3.84 times higher than the gravity force (see the last column in Table 2). For the experiment No. 3, the current density is 580 kA/m^2 . This induces the apparent supergravity almost 7 times stronger than the natural gravity. These values of LF density are calculated from formula (3).

The solidification process of the composite melt under conventional conditions, experiment No. 1, results in the structure which has a large content

of the reinforcing phase at the bottom of the ingot, small particle concentration in the middle region and almost zero particle concentration in the upper part of the ingot. This can be clearly seen in Fig. 18. Shrinkage and gas porosity can be observed in each region.

Table 2. Values of parameters used in experiments and calculated densities of Lorentz and gravitational forces for liquid F3S.10S composite ($f^G = \rho g$)

Experiment No.	j [kA/m ²]	S [m ²]	LF density, f^L [kN/m ³]	Gravity force density, f^G [kN/m ³]	f^L/f^G
1	0	270×10^{-6}	0	25	0
2	320	252×10^{-6}	96	25	3.84
3	580	207×10^{-6}	174	25	6.96

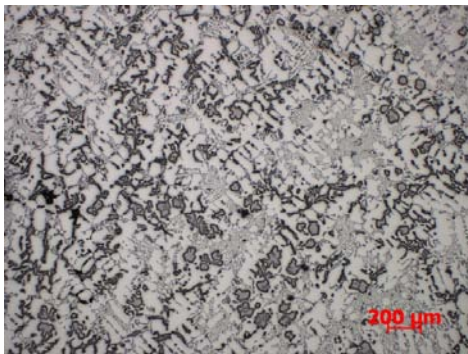
The distribution of reinforcing phase (SiC_p) is very different when solidification runs in Lorentz field. In the next two experiments the Lorentz force is directed downward. The electrical conductivity of the melt is relatively high whereas the electrical conductivity of SiC is in fact zero. Due to Lorentz field, this causes Archimedes force of a high value (see second term in the right member of (6)), which is acting upward. The solid particles of the reinforcing phase begin to float to the upper melt surface. This process is concurrent with solidification, and final particle distribution is determined by relationships that exist between the velocities of particles and the solid/liquid interface movement. Particle distribution in this case, experiment No. 2, is shown in Fig. 19. The reinforcing phase can be observed in every region of the ingot. The particles at the bottom are of a smaller size and occur in lower percentage. Higher percentage of the particles is observed in the middle region of the ingot. Shrinkage and gas porosity are concentrated predominantly in the top region but small amounts of gas bubbles can be observed also in the remaining regions of the ingot.



a)



b)

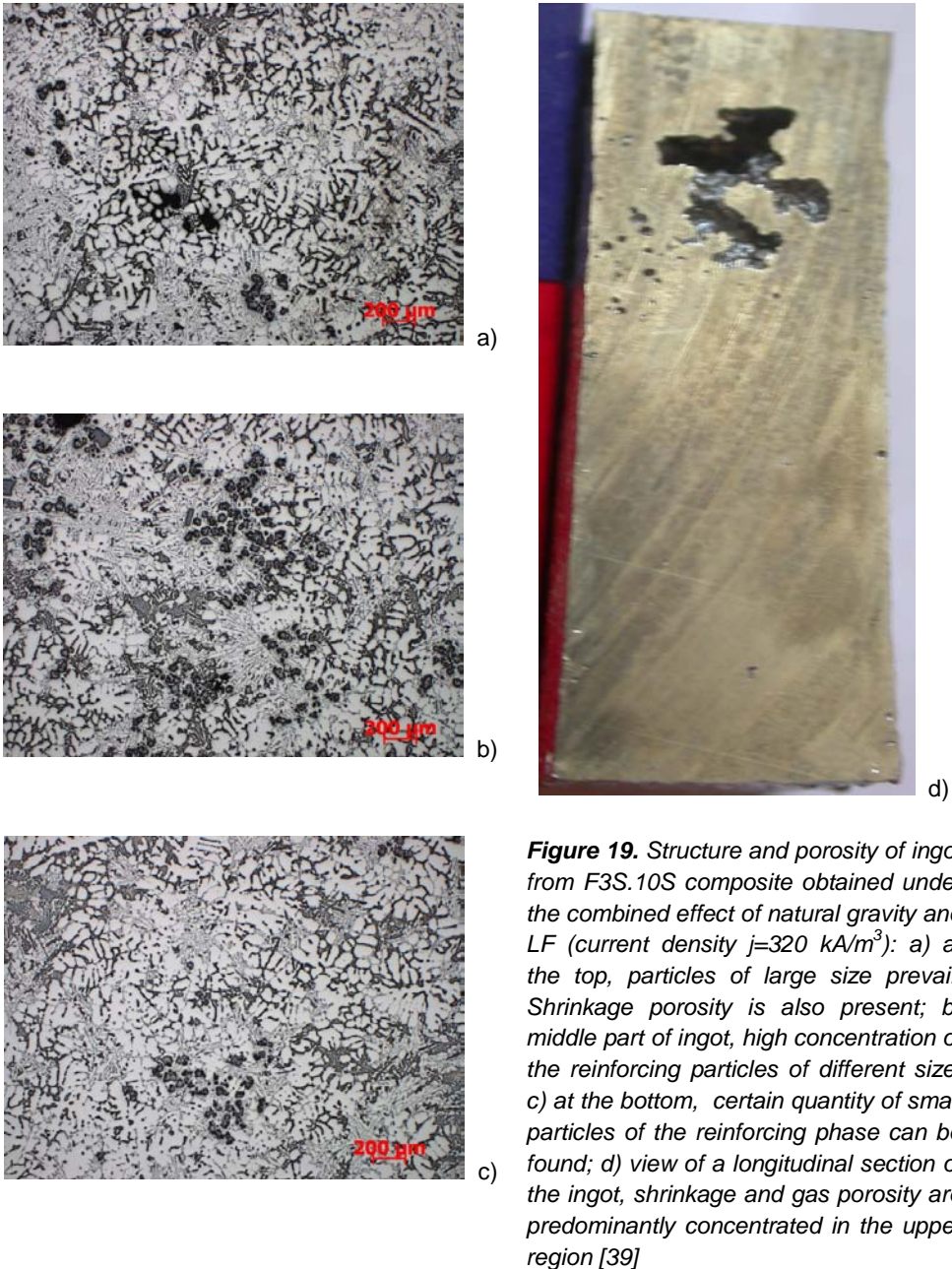


c)



d)

Figure 18. Structure and porosity of ingot from F3S.10S composite obtained under natural gravitational conditions: a) at the top, no particles of practical interest can be observed; b) middle part of ingot, only small isolated particles of the reinforcing phase are present; c) at the bottom, high concentration of the reinforcing phase; d) view of a longitudinal section of the ingot, shrinkage porosity can be found in the entire ingot volume [39]



When the Lorentz field is of higher intensity as in experiment No. 3, Fig. 20, a particle-rich zone is formed in the upper region of the ingot because the reinforced phase is floating rapidly to the top. Particles of large, medium and

small size can be observed in this region. In the middle region, the particles are predominantly of small size. There are no particles of practical interest in the bottom part of the ingot. The gas porosity is concentrated strongly in the top region.

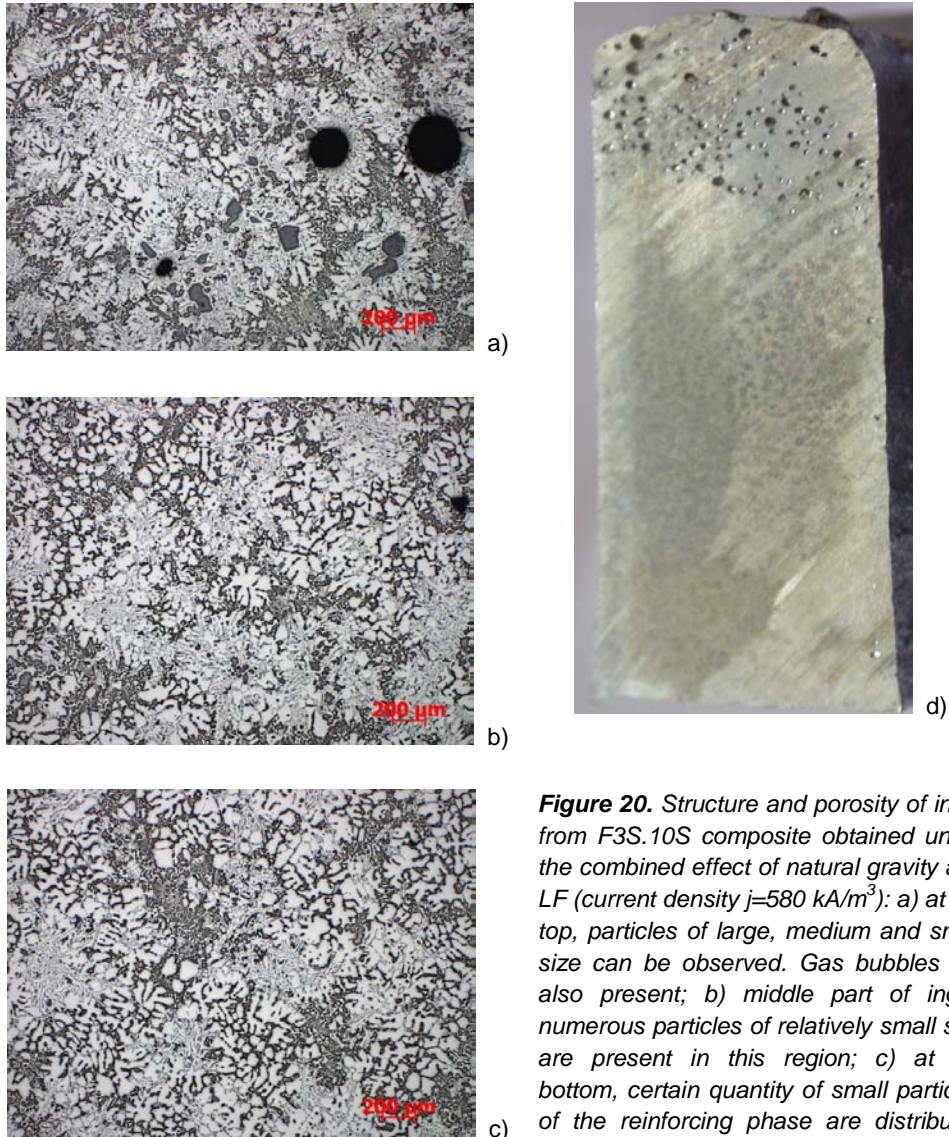


Figure 20. Structure and porosity of ingot from F3S.10S composite obtained under the combined effect of natural gravity and LF (current density $j=580 \text{ kA/m}^3$): a) at the top, particles of large, medium and small size can be observed. Gas bubbles are also present; b) middle part of ingot, numerous particles of relatively small size are present in this region; c) at the bottom, certain quantity of small particles of the reinforcing phase are distributed homogeneously; d) view of a longitudinal section of the ingot, porosity is strongly concentrated only in the upper region [39]

Our experience shows that higher electrical component in the LF causes more intensive vortical flow of the melt, especially close to the electrodes. If such a movement is not desired, to retain the same value of LF, one should decrease the density of the electric current and increase the intensity of the magnetic field. Another special feature of the method discussed here is the positive inverse relationship between the density of the electric current and vibrations in the upper surface of the melt. Each random melt vibration causes local changes in its cross-section, running perpendicular to the electric current. A reduction of the cross-section will cause local increase of the current density, which, in turn, will generate higher values of LF in this zone. The latter will amplify the vibrations of the melt and the wave-like moving of its surface. To avoid this instability in melt shape, closed ceramic molds should be used.

On the basis of the results discussed above it can be concluded that:

1. Application of Lorentz force during solidification allows control of both homogeneous and graded structures in particle reinforced MMCs and provides gradual transition from the particle-rich zones to the particle-free ones;
2. Lorentz force generated by crossed constant electric and magnetic fields can be used as an instrument for the in-situ control of MMCs structure;
3. The solidification under apparent supergravity conditions forces in a substantial degree the removal of gas inclusions to the upper part of ingot;
4. Lorentz field applied to electroconductive liquid mixtures provides an opportunity for non-mechanical separation and temporary storage of various inclusions with subsequent melt purification. The inclusions can be separated either on the top or on the bottom of the liquid volume. This is very important when sedimentation/flotation process is hindered due to approximately equal densities of different phases in the mixture.

IV.2. The planned experimental activities

In what follows some of the special experiments planned for the future will be discussed briefly. As it has been mentioned above, the intensity of Lorentz field depends on the mold or vessel geometry. It should be mentioned that, according to (3), the density of LF is proportional to the current density. If the vessel bottom is not flat as in Fig. 21, the current density in zone 1, above

the bottom peak, is greater than in zone 2, far from the peak, which results in more intensive Lorentz field in zone 1 than in zone 2. Because of this, due to Archimedes force, zone 2 will contain more particles (or contaminations) than zone 1. If the suspension is MMC melt, after solidification an ingot of graded particle distribution will be obtained. Different combinations of peak(s) height and position(s) will result in obtaining of ingots with graded structure. Regions of gradual reinforcing phase distribution can be controlled by simple variations in mold geometry. Moreover, the accumulation of a reinforcing phase in certain regions can avoid additional surface treatment. Because of this, our efforts will be focused on determination of basic relations between the mold shape and position of reinforced regions.

Analogous experiments can be carried out for purification of the base liquid. By means of a pipe submerged in zone 1, as is shown in Fig. 22, the “purified” base liquid can be transported out of the vessel. Such idea can be used for separation of the impurities from a liquid (if the pipe is submerged in zone 2), or for separation of different phases in a suspension or colloid.

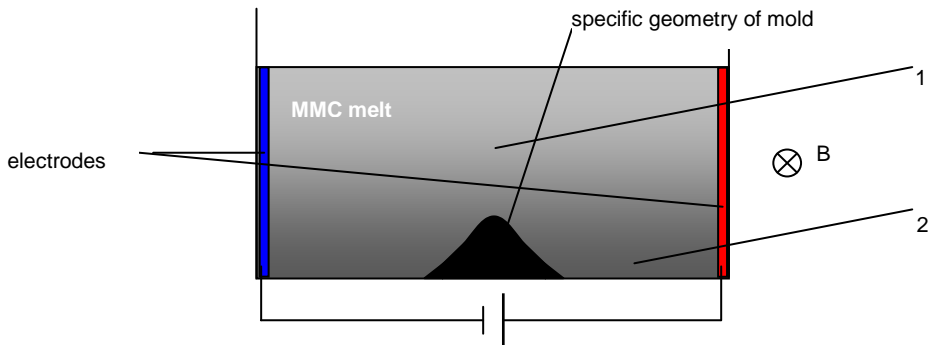


Figure 21. Mold with varied cross-section. The ingot will be reinforced in selected regions. Regions 1 and 2 contain different amounts of the reinforcing phase

Manipulation of gravity by LF can result in stimulation of the flotation or sedimentation processes. This is very important when the impurities or the second phase are of a density similar as the base liquid. Such a case of practical significance is liquid aluminum alloy and aluminum oxides dispersed in it. Experiments are planned to be conducted to obtain separation of different phases and subsequent removal of impurities. The experimental equipment looks as shown in Fig. 23. The outlet can be positioned in a lower or higher part of the vessel, depending on which phase we want to remove. A cascade design

of such system (many times repeated separation) will increase the effect of base liquid purification or second phase concentration.

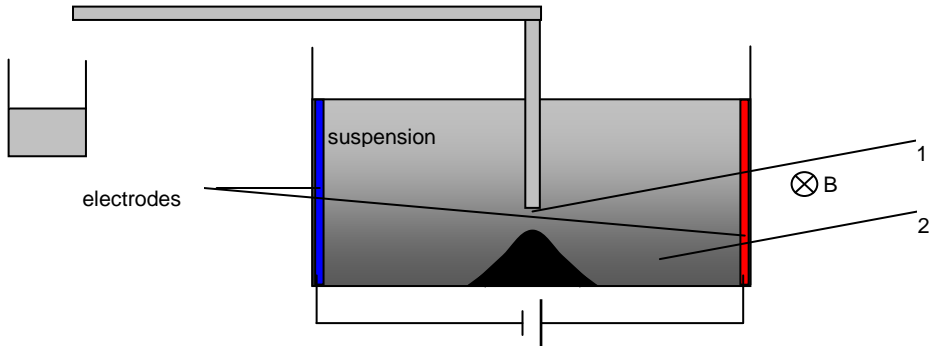


Figure 22. Transportation of “purified” base liquid. LF in the pipe is zero because the electric current density is zero. The pressure in the pipe is close to the atmospheric one while pressure in the liquid above the peak is higher due to LF. This causes the fluid flow through the pipe. Regions 1 and 2 contain different amounts of inclusions

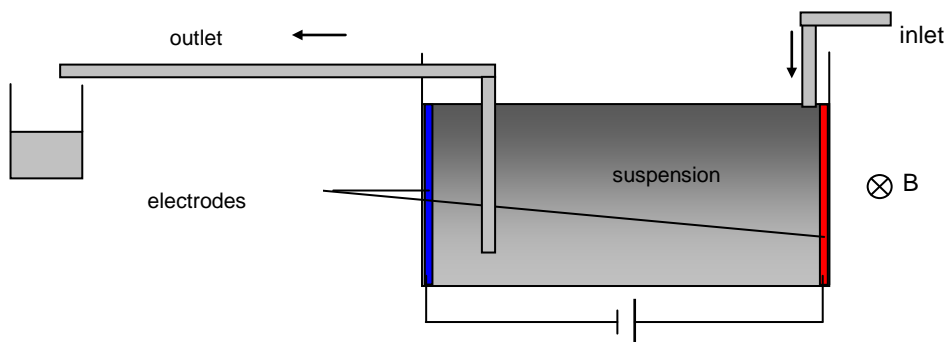


Figure 23. Principle diagram of system for continuous phase separation. Cascade design of this process will substantially improve the result

The effect of mold geometry reveals its potential in the formation of a trapezoidal composite ingot, Fig. 24. In this case the current density in the top region of the MMC melt will be smaller than the density in the down region. Because of this, the intensity of Lorentz field will be increasing from top to bottom and the slope of trapezoidal mold sides will define gradient of the

Lorentz field. There are physical reasons to expect a layered distribution of the secondary phases (if the reinforcing phase is mixture of different phases) in MMC ingot. The stratification is feasible by appropriate combination of the processing parameters and the slope of the mold sides. In this manner, a homogeneous or graded particles distribution can be produced in the ingot for two different types of particles.

The proposed “geometrical” approach promises to be fruitful for simultaneous separation of two phases dispersed in a base electroconductive liquid. If the two phases are of similar density it will be extremely difficult to separate them by conventional techniques. The experimental system as shown in Fig. 24 can be a solution of such problem.

Another geometrical variant which stimulates sedimentation is shown in Fig. 25. Here, if LF is directed upward, the inclusions of the electrical conductivity lower than the base liquid will settle quickly in the down region of the vessel. From this position they can be removed easily through special outlet. In this case, to avoid mixing in the suspension, a symmetry in respect to A-A plane (see Fig. 25) is strongly recommended.

Castings with triangular cross-section and graded distribution of reinforcing particles can be obtained by specific configuration shown in Fig. 26. The cavity of the ceramic mold is of a triangular cross-section and the electrodes are placed at its lateral sides. When the melt is subjected to LF which acts downward, the components of lower electrical conductivity will float upward. After completing of the solidification process they will form a layer with high content of the reinforcing phase which will be gradually decreasing towards the down part of the ingot.

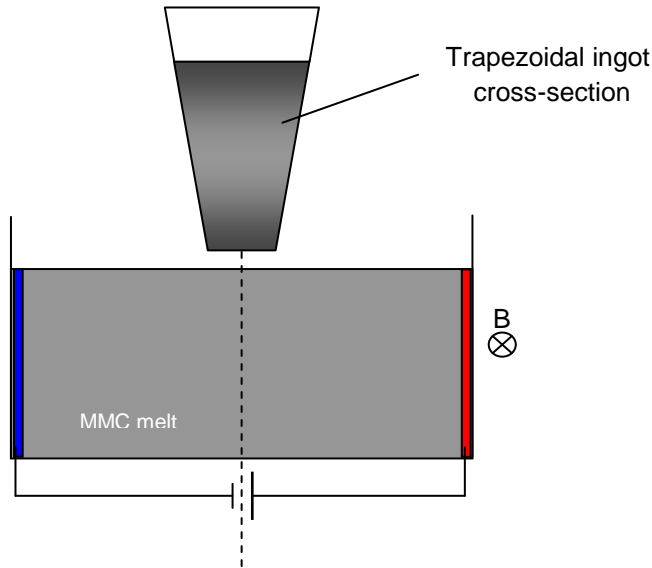


Figure 24. Mold with trapezoidal cross-section. This shape is suitable for control of the secondary phase distribution

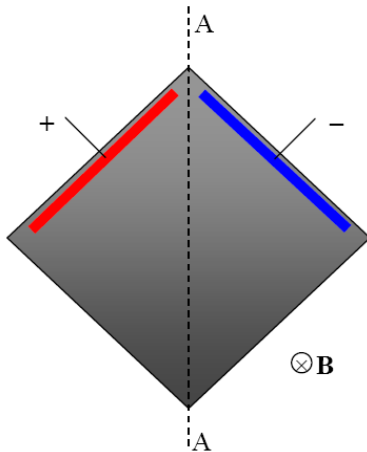


Figure 25. Principal chart of configuration which accelerates sedimentation in suspension

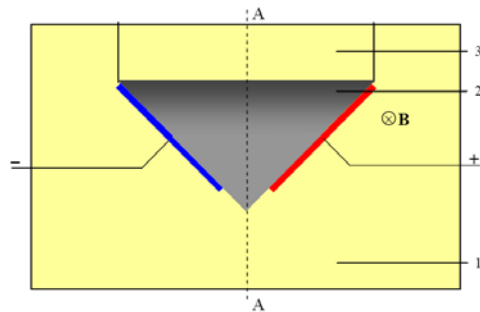


Figure 26. Principal chart of configuration which accelerates flotation in suspension: 1-ceramic mold; 2-casting; 3-ceramic cover

Various processing regimes will be tested to find the most effective parameters for additional mechanical treatment. Two types of plastic deformation – rolling and forging – will be tested to improve the physical properties of the graded materials obtained.

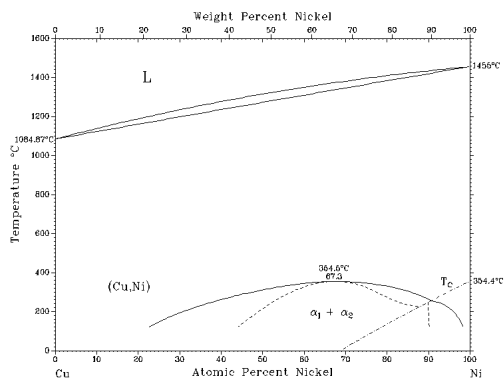
The macro- and micro-structure of the ingots obtained will be investigated by optical microscopy, and by SEM, TEM, EDS and XRD at both room and elevated temperatures.

Mechanical properties of the new materials will be determined. Micro hardness, tensile strength, yield strength and ultimate tensile strength will be measured by conventional methods and the respective stress-strain curves will be plotted.

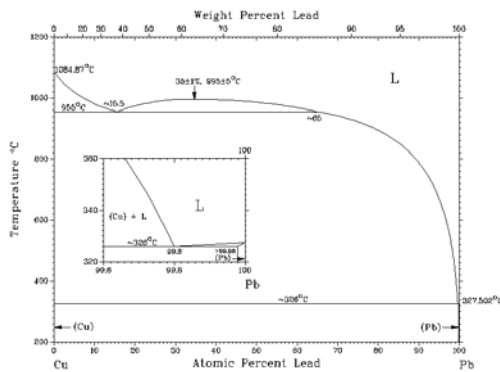
Thermal properties of the obtained materials are of major importance for their application. Heat conductivity will be measured in different regions of the graded materials. The integrated coefficient of thermal expansion will be determined over a large temperature range. It is also planned to find out what tribological properties the newly designed composite objects can offer.

It is very interesting to carry out experiments for the determination of surface tension and wettability as function of pressure at apparent supergravity and apparent microgravity. For this purpose we plan to use different combinations of immiscible liquids and substrates. Experiments of this type are intended to form an essential part of our study. Some binary phase diagrams are given in Fig. 27. The binary alloy with miscibility gap comprised in a very large temperature and concentration interval is Pb-Al alloy, Fig. 12 c). This fact makes it extremely suitable for the investigation of wettability phenomena in supergravity and microgravity. We would like to emphasize again the fact that such investigations will be of great importance and will have strong impact on the development of modern material science.

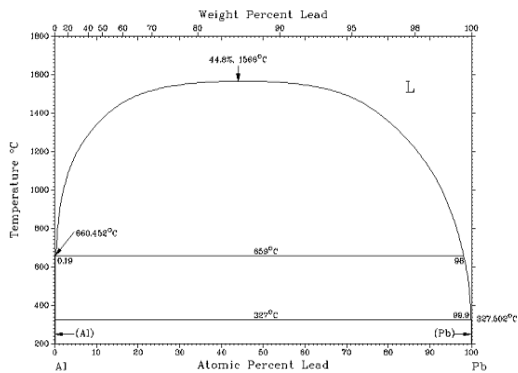
Thermal properties of the materials obtained are of major importance for their application. Heat conductivity will be measured in different regions of the graded structures. The integrated coefficient of thermal expansion will be determined over large temperature range. It is also planned to find out what tribological properties these new composite materials may have.



a)



b)



c)

Figure 27. Phase diagrams of binary systems with miscibility gaps: a) Cu-Ni system; b) Cu-Pb system; c) Al-Pb system with large miscibility gap

IV.3. Some theoretical considerations

Before specific experiments are conducted, it will be very useful to estimate the effects expected and to find appropriate processing parameters, all this in order to reduce time and cost of the experimental work. Below, the determination of critical value of the effective current density which provides zero gravity effect for solid particles in a suspension will be discussed. Numerical experiments for the evaluation of LF generated pressure in a drop and its effect on the drop shape will be also briefly commented.

IV.3.1. Determination of critical current density

Here we will determine the critical electric current density, j_{cr} , for which Archimedes force \mathbf{F}_A^L generated by LF and acting on single particle in a suspension is equal to Archimedes force \mathbf{F}_A^G generated by gravity and applied to the same particle. In this case, if the two forces are acting in opposite directions, $\mathbf{F}_A^L = -\mathbf{F}_A^G$, according to (6) the particle will not move, and apparent zero gravity will prevail. If the current density is greater than the critical one, $j > j_{cr}$, the apparent antigravity conditions are valid in the suspension considered, and the relation $j < j_{cr}$ indicates apparent supergravity (see Fig. 1.).

Let us consider a suspension of electroconductive liquid with spherical solid particles of volume $V_p = 4/3 \pi r_0^3$ and concentration ε . According to (5), the total LF that acts on the liquid of volume V_p is expressed by relation

$$\mathbf{F}_m^L = \sigma \mathbf{E} \times \mathbf{B} V_p \quad (31)$$

Total LF acting on a particle in the same position will be

$$\mathbf{F}_p^L = \sigma_p \mathbf{E} \times \mathbf{B} V_p \quad (32)$$

The resulting Archimedes force due to LF will be

$$\mathbf{F}_A^L = \mathbf{F}_m^L - \mathbf{F}_p^L = (\sigma - \sigma_p) \mathbf{E} \times \mathbf{B} V_p \quad (33)$$

The average electrical conductivity of the suspension can be expressed by the rule of mixture, i.e.

$$\sigma_{eff} = \varepsilon \sigma_P + (1 - \varepsilon) \sigma \quad (34)$$

and the electric current in the suspension is

$$\mathbf{j} = \sigma_{eff} \mathbf{E}. \quad (35)$$

Substituting \mathbf{E} from (35) in (33) we obtain

$$\mathbf{F}_A^L = \frac{(\sigma - \sigma_P)}{\varepsilon \sigma_P + (1 - \varepsilon) \sigma} \mathbf{j} \times \mathbf{B} V_P \quad (36)$$

The Archimedes force due to gravity is given by relation

$$\mathbf{F}_A^G = (\rho - \rho_P) \mathbf{g} V_P. \quad (37)$$

The critical value of the electric current results from relation $\|\mathbf{F}_A^L\| = \|\mathbf{F}_A^G\|$ which gives

$$j_{cr} = \frac{\varepsilon \sigma_P + (1 - \varepsilon) \sigma}{(\sigma - \sigma_P)} (\rho - \rho_P) \frac{g}{B} \quad (38)$$

In case of hyper-eutectic Al–Si alloy we can estimate j_{cr} for $B = 0.4\text{T}$ and $\varepsilon = 0.05$. Another parameters are as follow: $g = 9.81 \text{ m}\cdot\text{s}^{-2}$, $\sigma = 3.78 \times 10^7 \text{ }\Omega^{-1}\cdot\text{m}^{-1}$, $\sigma_P = 1.56 \times 10^{-3} \text{ }\Omega^{-1}\cdot\text{m}^{-1}$, $\rho = 2375 \text{ kg}\cdot\text{m}^{-3}$, $\rho_P = 2400 \text{ kg}\cdot\text{m}^{-3}$ (Si particles). The formula (38) gives for critical current density $j_{cr} = 490.5 \text{ A/m}^2$. The particle density is almost equal to the liquid alloy density and the electrical conductivity of the particle is almost zero. Because of this, the critical value of the current is so small. For AlSi7Mg alloy and 15 vol. % SiC_P $\rho_P = 3200 \text{ kg}\cdot\text{m}^{-3}$, $\varepsilon = 0.15$, $\sigma_P \sim 0 \text{ }\Omega^{-1}\cdot\text{m}^{-1}$, the formula (38) gives $j_{cr} = 17531 \text{ A/m}^2$.

The terminal velocity v can be determined from the relation

$$\|\mathbf{F}_s\| = \|\mathbf{F}_A^L\| - \|\mathbf{F}_A^G\| \quad (39)$$

which leads to

$$v = \frac{2r_0^2}{9\eta} \left(\frac{\sigma - \sigma_p}{\varepsilon\sigma_p + (1 - \varepsilon)\sigma} j B - (\rho - \rho_p)g \right). \quad (40)$$

In case of hyper-eutectic Al–Si and $j = 2 j_{cr}$, $\eta = 4.0 \times 10^{-7}$ Pa·s, $\rho = 2400$ kg/m³, $\rho_p = 2375$ kg/m³, $\varepsilon = 0.05$, $\sigma = 3.78 \times 10^7$ Ω⁻¹m⁻¹, $\sigma_p = 1.56 \times 10^3$ Ω⁻¹m⁻¹, $r_0 = 1.0 \times 10^{-4}$ m the terminal velocity is about $v = 0,014$ m/s.

IV.3.2. Numerical experiments with electroconductive drops

The purpose of such experiments is to find how electromagnetically induced elevated pressure affects the wettability and other phenomena in immiscible metallic melts. The mathematical problem can be defined in the following way: to consider electroconductive liquid and drops of different shapes in configuration shown in Fig. 28. This liquid is placed in constant magnetic and electric fields which are perpendicular. If all needed electrical and geometrical parameters are known, to determine LF field in the liquid and in the drops.

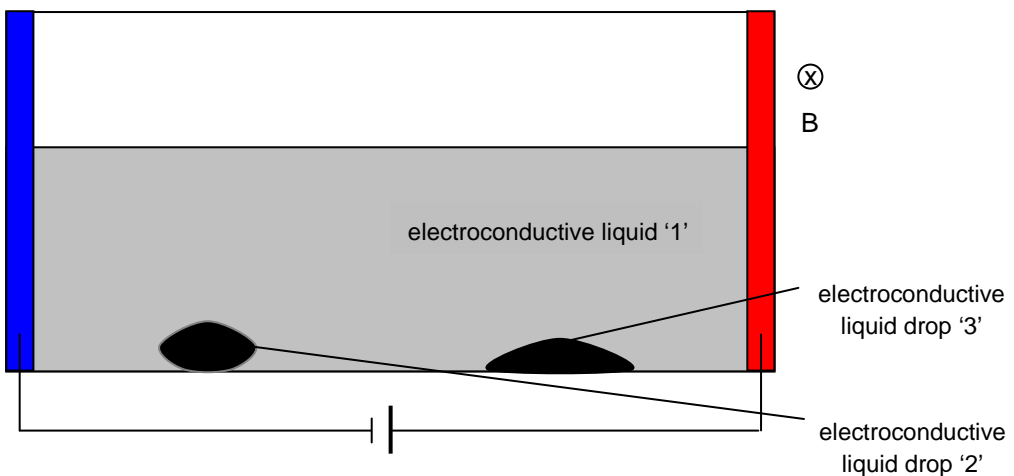


Figure 28. Principal chart of physical configuration related with the problem

It is intended to use a commercial software product like ANSYS or similar one. The calculations must be carried out for various combinations of the electrical conductivity and density of the drop and base liquid. The obtained values and directions of the LF field will give information on what changes in the shape and position of the drops can be expected due to this additional field. We believe this will be useful in search for other practical applications.

V. Expected results and their practical applications

The applied aspects of the project here discussed consist of:

1. New MMCs of functionally graded structure and properties will be obtained;
2. Large investigation of specific structure and some mechanical properties of the materials obtained will be carried out;
3. Samples for determination of effective plastic processing, which improves the graded composite structure and properties will be prepared.

Possible implementations of the project results can be realized in two lines: first, production of specific MMCs which cannot be obtained by conventional casting methods, and second, phase separation in various suspensions and colloids used by metallurgy, chemistry, pharmacy and others.

The **first line** comprises manufacturing of various cast parts from particulate reinforced MMCs with graded or homogeneous structure. (Let it be mentioned and stressed once again that the approach adopted in this project is equally well applicable in producing both graded and homogeneous particle distributions in metal melt, depending on the specific processing parameters.) Castings can be reinforced in some regions, while being entirely free from the reinforcing phase in the others. Such requirements are imposed on certain machine elements operating in automotive and military industries, on medical tools, sport equipment and others. The method considered offers various possibilities to meet these requirements by flexible combination of the magnitude and direction of the electric current and magnetic field with mold geometry.

Another original application of the project results can be obtaining of controllable homogeneous or layered particle distribution in MMC volume when the reinforcing phase contains two types of particles. Examples of such

complex MMCs are aluminum- or copper-based alloys used as a matrix mixed with graphite and SiC_P particles as a reinforcing phase. The idea lying behind this concept is to combine “hard” mechanical properties of SiC_P with “soft” lubricating properties of graphite. It is believed that the method here considered holds a large potential for the manufacture of innovative MMCs for specific industrial applications.

The **second line** of potential applications is consistent with the possibilities of phase separation in various electroconductive suspensions and colloids. This approach is very effective when the liquid mixture contains components of similar densities. In this case the sedimentation and flotation processes are negligible. Very often, the centrifugally stimulated phase separation is inapplicable. Filtration is not always usable or generates insurmountable technical problems as in the case of liquid aluminum alloys with buoyant aluminum oxides present in them. By means of LF these problems can be overcome because LF is proportional to the specific electroconductivity but not to the specific mass (density) and inclusions can be moved to appropriate regions of the liquid volume and eliminated.

Controllable separation of different phases in liquid mixtures allows elaborating a set of various techniques not only for purification of liquid substances but also for homogenization of liquid solutions. Such techniques are a valuable tool for use in the chemistry and pharmacy. Application in foundry practice will be focused on the development of a new-type technology for metal melts purification and obtaining super purity metals for special uses. It is possible for the approach here discussed to contribute to the development of new ideas in “green technologies”.

One of the problems arising in MMCs application is that they cannot be used as raw material. The main reason that accounts for this fact is the lack of a technology that would enable the utilization and reuse of MMCs waste and especially of the particulate reinforced metallic matrix composites. The approach considered in this project is very promising in this respect. The elaboration of technology for rapid phase separation in liquid composite slurry could be of great importance for the foundry practice and metallurgy in general. Possible reuse of metallic composite materials will reduce the total price of MMCs production.

All the experiments described above are of a unique character and therefore some of the results are unpredictable. But there is no doubt that the expected results and the elaborated technologies can be of great importance and can discover an innovative area in the field of new materials design. All possibilities for patent claims will be explored.

Symbols

- B** – magnetic field, T
 C_{eff} – effective heat capacity, J·K⁻¹
 C_P – heat capacity, J·K⁻¹
E – electric field strength, V·m⁻¹
 f_L – liquid fraction in two-phase zone, –
 \mathbf{f}^L – volume density of Lorentz force, N·m⁻³
 \mathbf{F}^L – Lorentz force acting on charged point particle, N
 \mathbf{F}_S – drag force (Stokes force), N
 \mathbf{F}_A^L – Archimedes force due to Lorentz field, N
 \mathbf{F}_A^G – Archimedes force due to gravity, N
 \mathbf{F}_B^G – buoyant force due to gravity, N
 \mathbf{F}_P^G – gravity force acting on point particle, N
 \mathbf{F}_B^L – buoyant force due to Lorentz field, N
 \mathbf{F}_P^L – Lorentz force acting on point particle, N
g – the gravitational acceleration, m·s⁻²
L – Lorentz field strength, V·T·m⁻¹
j – electric current density, A·m⁻²
 m_p – mass of particle, kg
 n – density of free electrons in a metal, 1·m⁻³, $n = 10^{28}$
 p – pressure, Pa
 q – electrical charge of point particle, C
 r_0 – particle radius, m
 t – time, s
 T_L – liquidus temperature, K
 T_S – solidus temperature, K
 T_{Cr} – critical temperature, K
 T_1, T_2, T_3, T_4 – ambient temperature, K
v – instantaneous velocity, m·s⁻¹
 V – volume of measured space, m³
 V_p – volume of particle, m³
 x, y, z – Cartesian coordinates, m
 $\alpha_1, \alpha_2, \alpha_3, \alpha_4$ – heat exchange coefficients, W·m⁻²·s⁻¹
 ε – fraction of solid particles in suspension, –
 η – apparent viscosity of suspension, Pa·s
 η_0 – dynamic viscosity of melt, Pa·s
 λ – thermal conductivity, W·m⁻¹·K⁻¹
 μ – magnetic permeability, H·m⁻¹
 ρ – melt density, kg·m⁻³
 ρ_p – particle density, kg·m⁻³
 σ – specific electrical conductivity of melt, Ω^{-1} ·m⁻¹
 σ_p – specific electrical conductivity of particle, Ω^{-1} ·m⁻¹
 σ_{eff} – specific electrical conductivity of suspension, Ω^{-1} ·m⁻¹

References

1. O. Darrigol, *Electrodynamics from Ampère to Einstein*. Oxford: Oxford University Press, (2000) p. 327. ISBN 0-198-50593-0
<http://books.google.com/?id=ysMf2pAid94C&printsec=frontcover&dq=Electrodynamics>
2. G. Hulot, A. Chulliat, On the possibility of quantifying diffusion and horizontal Lorentz forces at the Earth's core surface, *Physics of the Earth and Planetary Interiors* **135** (2003) pp. 47-54.
3. T. F. Dehel, M. Dickinson, F. Lorge, R. Startzel Jr., Electric field and Lorentz force contribution to atmospheric vortex phenomena, *Journal of Electrostatics* **65** (2007) pp. 631-638.
4. P. Lehmann, R. Moreau, D. Camel, R. Bolcato, Modification of interdendritic convection in directional solidification by a uniform magnetic field, *Acta Materialia* **46** (11) (1998) pp. 4067-4079.
5. Xi Li, Y. Fautrelle, Z. Ren, Influence of an axial high magnetic field on the liquid–solid transformation in Al–Cu hypoeutectic alloys and on the microstructure of the solid, *Acta Materialia* **55** (2007) pp. 1377-1386.
6. Xi Li, A. Gagnoud, Z. Ren, Y. Fautrelle, R. Moreau, Investigation of thermoelectric magnetic convection and its effect on solidification structure during directional solidification under a low axial magnetic field, *Acta Materialia* **57** (2009) pp. 2180-2197.
7. Xi Li, Y. Fautrelle, Z. Ren, Influence of thermoelectric effects on the solid–liquid interface shape and cellular morphology in the mushy zone during the directional solidification of Al–Cu alloys under a magnetic field, *Acta Materialia* **55** (2007) pp. 3803-3813.
8. Xi Li, Y. Fautrelle, Z. Ren, Morphological instability of cell and dendrite during directional solidification under a high magnetic field, *Acta Materialia* **56** (2008) pp. 3146–3161.
9. Xi Li, Y. F., Z. Ren, A. Gagnoud, R. Moreau, Y. Zhang, C. Esling, Effect of a high magnetic field on the morphological instability and irregularity of the interface of a binary alloy during directional solidification, *Acta Materialia* **57** (2009) pp. 1689-1701.
10. Xi Li, Z. Ren, Y. Fautrelle, Y. Zhang, C. Esling, Morphological instabilities and alignment of lamellar eutectics during directional solidification under a strong magnetic field, *Acta Materialia* **58** (2010) pp. 1403-1417.
11. Xi Li, Y. Zhang, Y. Fautrelle, Z. Ren, C. Esling, Experimental evidence for liquid/solid interface instability caused by the stress in the solid during directional solidification under a strong magnetic field, *Scripta Materialia* **60** (2009) pp. 489-492
12. B. Zhang, J. Cui, G. Lu, Effect of low-frequency magnetic field on macrosegregation of continuous casting aluminum alloys, *Materials Letters* **57** (2003) pp. 1707-1711.
13. I. Egry, Structure and properties of levitated liquid metals, *Journal of Non-Crystalline Solids*, 250-252 (1999) 63-69.

14. I. Egry, J. Brillo, D. Holland-Moritz, Yu. Plevachuk, The surface tension of liquid aluminium-based alloys, *Materials Science and Engineering A* **495** (2008) 14-18.
15. I. Egry, G. Jacobs, D. Holland-Moritz, EXAFS investigations on quasi-crystal-forming melts, *Journal of Non-Crystalline Solids* **250-252** (1999) 820-823.
16. D. Holland-Moritz, G. Jacobs, I. Egry, Investigations of the short-range order in melts of quasicrystal-forming Al-Cu-Co alloys by EXAFS, *Materials Science and Engineering* **294-296** (2000) 369-372.
17. J. Brillo, A. Bytchkov, I. Egry, L. Hennem, G. Mathiak, I. Pozdnyakova, D.L. Price, D. Thiaudiere, D. Zangh, Local structure in liquid binary Al-Cu and Al-Ni alloys, *Journal of Non-Crystalline Solids* **352** (2006) 4008-4012.
18. I. Egry, D.M. Herlach, L. Ratke, M. Kolbe, D. Chatain, S. Curoitto, L. Battezzati, E. Johanson, N. Pryds, Interfacial properties and solidification of immiscible Co-Cu alloy, *High Temperature capillarity*, Athens 2009, in print.
19. Y.K. Zhang, J. Gao, D. Nagamatsu, T. Fukuda, H. Yasuda, M. Kolbe, J.C. He, Reduced droplet coarsening in electromagnetically levitated and phase-separated Cu-Co alloys by imposition of a static magnetic field, *Scripta Materialia* **59** (2008) pp. 1002-1005.
20. Koizumi M., Niino M., *MRS Bull.* **20 (1)** (1995), pp. 19-24.
21. Mortensen A., Suresh S., *Int. Mater. Rev.* **40** (1995), pp. 239-246.
22. Sobczak J., Drenchev L., *Functionally Graded Materials (Processing and Modeling)*, Foundry Research Institute, Krakow, Poland, ISBN 978-83-88770-31-9 (2008). (See also J. Sobczak, L. Drenchev, *Metal Based Functionally Graded Materials (Engineering and modeling)*, Bentham Science Publisher, ISBN: 978-1-60805-038-3, 2009. <http://www.bentham.org/ebooks/9781608050383/index.htm>)
23. D. Kopeliovich et al., US Patent 6 273 970 B1, Aug., 14 2001.
24. C.J. Song, Z.M. Xu, J.G. Li, *Mater. Sci. Eng. A* **445-446** (2007) pp. 148-154.
25. S. Asai, *Sci. Technol. Adv. Mater.*, **1** (2000) pp. 191-200.
26. C.J. Song, Z.M. Xu, G. Liang, J.G. Li, *Mater. Sci. Eng. A* **424** (2006) pp. 6-16.
27. K. Mazuruk, *Adv. Space Res.* **29** (4) (2002) pp. 541-548.
28. A. Katsuki, I. Uechi, Y. Tanimoto, *Bull. Chem. Soc. Jpn.* **77** (2004) pp. 275-279.
29. C.J. Song, Z.M. Xu, X. Liu, G. Liang, J.G. Li, *Mater. Sci. Eng. A* **393** (2005) pp. 164-169.
30. B. Fischer et al., *Proc. EMP 2000* (2000) pp. 497-502.
31. W. Lesniewski, P. Wieliczko, P. Darlak, L. Drenchev J. Sobczak, Arrangement of particle distribution in Al-Si/SiCP composite by means of Lorentz force, *International conference Cast Composites, CC'09*, Kielce, Poland, 11-14 October 2009, in print.

32. D. Uffelmann, W. Bender, L. Ratke, B. Feuerbacher, Ostwald ripening in Lorentz-force stabilized Cu-Pb dispersions at low volume fractions. I – experimental observations, *Acta metall, mater.* **43** (1) (1995) pp. 173-180.L. Drenchev, J. Sobczak, N. Sobczak, Sedimentation Phenomenon and Viscosity of Water – SiC Suspension under Gravity Condition – a Water Model Study for Composites Synthesis, *Colloids and Surfaces A* **197** (2002) pp. 203-211.
34. L. Drenchev, J.Sobczak, S.Malinov, W.Sha, Numerical Simulation of Macrostructure Formation in Centrifugal Casting of Particle Reinforced Metal Matrix Composites. Part 1: Model Description, *Modelling Simul. Mater. Sci. Eng.* **11** (2003) pp. 635-649.
35. L. Drenchev, J. Sobczak, N. Sobczak, W. Sha, S. Malinov, A comprehensive model of ordered porosity formation, *Acta Materialia*, **55** (19) (2007) pp. 6459-6471.
36. P. Barral, A. Bermúdez, M.C. Muñiz, M.V. Otero, P. Quintela, P. Salgado, Numerical simulation of some problems related to aluminium casting, *Journal of Materials Processing Technology* **142** (2003) pp. 383-399.
37. I. H. Katzarov, Finite element modeling of the porosity formation in castings, *International Journal of Heat and Mass Transfer*, **46** (9) (2003) pp. 1545-1552.
38. D. Pal, B. Talukdar, Buoyancy and chemical reaction effects on MHD mixed convection heat and mass transfer in a porous medium with thermal radiation and Ohmic heating, *Commun Nonlinear Sci Numer Simulat* **15** (2010) pp. 2878-2893. doi:10.1016/j.cnsns.2009.10.029.
39. W. Lesniewski, K. Daskdov, P. Wieliczko, P. Darlak, L. Drenchev, J. Sobczak, Use of Lorentz Force for Synthesis of Functionally Graded Materials, *Journal of Materials Science and Technology*, **18** (1) (2010), pp. 3-20.

